Brain stains: optimization of immunohistochemical methods for cleared thick neural tissue

Honors Thesis
Presented to the College of Agriculture and Life Sciences
Cornell University
In Partial Fulfillment of the Requirements for the Biological Sciences Honors Program

By
Mackenzie Lemieux
May 2018
Dr. Melissa Warden

Brain stains: optimization of immunohistochemical methods for cleared neural tissue

Mackenzie Lemieux

Department of Neurobiology and Behavior, Cornell University

Populations of GABAergic interneurons in the prefrontal cortex have been implicated in control and coordination of complex behaviors such as motivation and decision-making. Although the functions of each of the main GABAergic subtypes, SST, PV, and VIP, have been extensively investigated independently, a lack of techniques allowing simultaneous recording has precluded the ability to characterize the interactions between these cell types. Staining for markers of GABA cell types in thick tissue, and relating identities back to in vivo recordings, will allow explicit and direct characterization of how activity covaries in these populations. However, there has been minimal success when staining for GABAergic subtypes in thick tissue. I interrogated the different factors that might be affecting successful thick tissue staining using the Cuboid Method which enables controlled and efficient thick tissue preparation, staining, and experimental testing. Fixation, with both paraformaldehyde and glutaraldehyde, was observed to be a major factor influencing the ability of different SST, PV, and VIP antibodies to label their epitopes in thick tissue. Additionally, fixation appeared to affect SST and VIP staining differently than PV staining. SDS treatment prior to staining was shown to be compatible with GABAergic subtype staining while SDS treatment after staining was shown to dramatically decrease staining signal. Like others' findings, blocking was shown to be unnecessary for better PV and SST staining. Lastly, relative proportions of SST, PV, and VIP in the PFC and their staining patterns in thick tissue matched results from previous work in thin tissue to support that staining was successful and also accurate. This research provides the knowledge necessary to successfully stain for SST, PV, and VIP in thick tissue in addition to showing the efficacy of the Cuboid Method for testing factors affecting staining in thick tissue.

Introduction

The prefrontal cortex (PFC) coordinates highly complex behaviors such as decision-making, planning, and motivation[1,2]. In order to coordinate such complex tasks, the PFC has a wide variety of outputs including the amygdala[3], the ventral tegmental area, the dorsal raphe nucleus, and the lateral habenula[4]. The PFC circuits and their many outputs are implicated in emotional processing, reward valuation, addiction, and even depression, emphasizing the importance of further exploration of the PFC network[2]. The importance of understanding more about the PFC and the cell types that make up the many inhibitory circuits within it inspired this study which explores an optimized method to immunohistochemically probe for specific GABA neurons in thick tissue sections of the mouse PFC. The method I have optimized allows for identification of GABA neurons that were active during performance of sensory stimulation tasks.

Recent studies have shown that GABA interneurons in the PFC play an integral role in coordinating goal-directed behavior through both microcircuits and projection tracts to downstream structures[5]. There are three major categories of GABA interneuron subtypes in the PFC; these differentially express either the neuropeptide Somatostatin (SST), the calcium binding protein Parvalbumin (PV), or the neuropeptide Vasoactive Intestinal Peptide (VIP)[5–7]. While PV mainly functions in the cytosol to regulate calcium concentrations[8] both SST and VIP have neuromodulatory effects on postsynaptic neurons. SST has been shown to modulate the voltage dependent potassium current in postsynaptic neurons[9] whereas VIP has been shown to increase cAMP levels in downstream neurons[10]. Previous research has elucidated the different functions of these molecularly distinct subtypes defined by expression of SST, PV, and VIP. Using a go/no-go sensory stimulations task, mice were trained to lick for water based on a sensory stimulus[5].

Individual recordings of neural activity in SST, PV, and VIP interneurons showed correlations to distinct behaviors. The SST interneurons were shown to have the highest Ca^{2+} activity at the onset and ending of licking thus indicating that these neurons are implicated in motor-related activity[5]. The PV interneurons were found to have high Ca^{2+} activity at the onset and ending of licking, in response to rewarding trial outcomes, and in response to an auditory stimulus thus this subpopulation is implicated in a broad range of task related events[5]. The VIP interneurons were shown to have high Ca^{2+} activity in response to both rewarding and punishing task outcomes and thus were determined to be specialized to respond to task outcomes[5]. While the aforementioned study was limited to individual recordings, the tools optimized in my study will allow for simultaneous recordings of multiple GABA subtypes, whose activity can be correlated to behavior in unison.

It will be difficult to understand how the brain works if research is focused on individual populations of cells, single projections, or isolated brain areas without simultaneously considering the many other interconnected structures that are integral to brain function. The brain is a complex network with billions of connections between cells. There has been a recent increase in research on neural activity at the circuit or system level as the importance of neural connections is realized. For example, O'Hare et al.[11] showed that studying two striatal circuits simultaneously was more powerful at explaining behavior than studying a single circuit in isolation. They recorded indirect and direct striatal projection neurons from the dorsolateral striatum and found that habitual behavior correlated with Ca^{2+} activity (indicating neural activity) when both indirect and direct circuits were recorded simultaneously but not when they were recorded individually[11]. The function of the GABA interneurons in the PFC can be better understood through simultaneously

recording all three GABA subtypes and correlating their activity to behavior in a sensory stimulation task. Before in vivo imaging and behavioral studies recording from multiple cellular populations can be undertaken, the challenge of labelling three different types of GABA neurons in thick tissue must be tackled.

Immunohistochemistry is a common way to identify the molecular characteristics of neurons and will be used in this study to identify GABA neuron subtypes. To date, very little research has focused on staining for GABA interneuron subtypes in thick tissue. Allen et al.[12] successfully stained for both PV and SST in 100μm thick sections, while Tomer et al.[13] stained for both PV and SST in 1mm thick tissue. In this study, I stained for the three major GABA subtypes, SST, PV, and VIP, in 2mm thick tissue. I hypothesize that optimized immunohistochemistry techniques in cleared thick tissue to probe for the three major GABA interneuron subtypes simultaneously will allow for identification of neurons after they have been endoscopically imaged. In this way, the activity of neurons that are imaged while the mouse was alive can be molecularly characterized after death. Thick tissue would be preferred to thin sections for this experiment since it can best capture all recorded neurons and increase ease of alignment after staining. The thin section technique would make it more difficult to discern the location of endoscopically imaged cells since the lens has a large working distance (about 250μm) compared to the width of a thin tissue section[14]. Large volume data sets can provide more information about alignment of cell populations and allow for easier visualization of projections and tracts[15]. Despite the increased ability to capture and align cells, there are many difficulties that exist when working with thick tissue compared to thin tissue.

Thick tissue has two main limitations in the scope of this study: optical transparency and antibody penetration. To tackle the first limitation, I used a combination of lipid removal and immersion in refractive index matching solution. Lipid removal, also known as tissue clearing, is a process that removes lipids that impair the path of light through the tissue[15,16]. The process of clearing enables large volume samples to be more transparent deep in the tissue[16]. Some techniques that have been developed to clear tissue include CLARITY, iDISCO, CUBIC, ClearT, and FRUIT[16]. I used a clearing method adapted from Chung and Deisseroth's[15] technique called CLARITY, in which sodium dodecyl sulfate (SDS) is the main reagent that removes lipids. Refractive index matching solution is another integral component of achieving optical transparency as it prevents refraction and excess light scattering within the tissue[16]. Iodixanol, the refractive index matching solution used in this study, has been shown to produce high quality deep imaging in uncleared thick tissue[17]. Chung and Deisseroth[15] have shown the power of the CLARITY technique to allow for both deep imaging and immunohistochemical staining since removing lipids makes tissue more penetrable to antibodies. iDISCO is another method[18] designed to both clear thick tissue and increase antibody staining abilities. However, only certain antibodies are compatible with this technique, limiting the number of targets that can be probed for. With a limited number of tested antibodies, the second limitation was tackled by optimizing a protocol to stain thick tissue with each of the GABA interneuron antibodies: PV, SST, and VIP.

Optimizing a thick tissue staining protocol involves many factors including fixation type and duration, clearing reagents, target epitope, antibody choice, duration of stain, and duration of wash. Fixation, which is done to maintain tissue structure, often impairs antibody staining by forming cross-links that impede immuno-recognition of epitope by the antibody[19]. In addition, antibody-

fixative interactions vary based on epitope and antibody; thus, these factors must be carefully considered when trying to optimize an antibody in thick tissue[19]. Testing the many variables that impact thick tissue staining requires an immense amount of time since diffusion of antibodies and wash solution through thick tissue is slow. The larger the distance over which diffusion takes place, the longer diffusion takes based on Fick's Second Law in which diffusion rate is inversely proportional to the distance particles must travel[20]. In addition, the quantity of reagents needed to process and label thick tissue is drastically increased due to increased sample volume. To address slow diffusion time and large reagent quantities, I developed a technique that allowed for efficient immunohistochemical variable testing for many different PV, SST, and VIP antibodies. The technique involves small tissue chunks called cuboids. Brains were cut into 2mm thick sections, then cut again into eight cuboids. The cuboids enable controlled experimentation through matched anatomical pairs from each 2mm brain section. The left cuboid served as the experimental control, while the right cuboid was subjected to the experimental variable. Matched samples of cuboids from the same brain also allowed many antibodies to be tested in the context of varying reagent conditions. This tool is useful for testing antibodies prior to large thick tissue experiments in the future.

Through the use of the cuboid technique, six SST, three PV, and two VIP antibodies were tested in thick tissue. The efficacy of each antibody was first tested in thin section. Successful antibodies were then tested in thick sections using the same reagent conditions as in thin sections. The effects of SDS, Glutaraldehyde, and Glycine on antibody staining were tested. Antibody accuracy was then tested for one SST and one PV antibody in transgenic SST-cre TdTom and PV-cre TdTom mice. Overlap between transgenic expression of interneuron markers and immuno-labelling of

interneuron markers was observed. The successful thick tissue staining with SST, PV, and VIP GABA interneuron subtype antibodies lays the foundation for in vivo calcium imaging in which behavior can be correlated to simultaneous GABA interneuron activity in the PFC.

The relationship between relative GABA subtype firing and behavior will be explored through endoscopic in vivo calcium imaging of Vgat-Cre GCaMP6 mice while they perform a go/no-go sensory stimulation task similar to that performed by Pinto and Dan[5]. A cube of brain tissue that contains the recorded cells will be extracted from the brain and stained with PV, SST, and VIP antibodies to discern which GABA neurons correspond to which subtypes. The calcium imaging data can then be aligned with the cell staining results using an image alignment program. Interneuron activity can then be related to behavior within one mouse to understand how patterns of GABA interneuron firing predict observed behavioral outputs.

Materials and Methods

Transgenic mice and handling.

Transgenic mice were maintained and bred at Cornell following accepted IACUC policies. A total of 4 C57B6J, 3 SST-TdTomato-Cre Thy1-YFP mice, and 4 PV-TdTomato-Cre Thy1-YFP mice were used in the following experiments. SST-TdTomato-Cre Thy1-YFP mice and PV-TdTomato-Cre Thy1-YFP mouse lines were created at Cornell from Jackson Laboratories transgenic SST-Cre and PV-Cre lines. Mice were housed in groups and maintained on a 12hr/12hr light-dark cycle.

Perfusion.

8-week-old mice were anesthetized with pentobarbital at a dose of 65mg/kg. Once deeply anesthetized, the mice were placed on the perfusion platform in the fume hood. An incision was made in the abdomen with dissection scissors to expose the peritoneal cavity. Incisions were extended up both the right and left sides of the abdomen and thoracic cavity to expose the heart. A small incision was made in the right atrium and a 25 gauge needle was then inserted into the left ventricle. The circulatory system was perfused at a rate of 5mL/min with 20mL of 0.5% Heparin Nitrite in PBS. The circulatory system was then perfused with 20mL of 4% paraformaldehyde in PBS at 5mL/min. Brains were dissected and drop fixed overnight in 4% paraformaldehyde at 4°C. Brains were then dehydrated for cryoprotection in 30% sucrose at 4°C for 18 hours.

Thin tissue preparation and immunohistochemistry.

Fixed and dehydrated brains were then placed on the microtome, frozen with dry ice, and sliced into 50μm coronal sections. Three sections that included the prefrontal cortex (one rostral, one medial, and one caudal) were placed in a 40mL glass vial and washed with PBST. This was repeated to prepare one vial for each antibody. Sections were blocked for one hour at room temperature in 10% Normal Donkey Serum (NDS) in PBST or 10% Normal Goat Serum (NGS) in PBST to match the secondary antibody. After blocking, primary antibodies (Chicken anti-SST 3:1000, SYSY; Rat anti-SST 3:1000, Millipore; Mouse anti-SST (H-11) 3:1000, Santa Cruz Biotechnology Inc.; Rat anti-SST (YC7) 3:1000, Santa Cruz Biotechnology Inc.; Mouse anti-SST (D-12) 3:1000, Santa Cruz Biotechnology Inc.; Mouse anti-VIP (H-6) 3:1000, Santa Cruz Biotechnology Inc.; Mouse anti-SST (G-10) 3:1000, Santa Cruz Biotechnology Inc.) were diluted in 5% Normal Donkey Serum in PBST or 5% Normal Goat Serum in PBST and the sections were

incubated overnight at room temperature. Sections were then washed in PBST at room temperature for 1, 5, and 10 minutes. The secondary antibodies (Donkey anti-Rat Alexa Fluor 647 3:400, Invitrogen; Goat anti-Mouse IgG1 Fluor 647 3:400, Invitrogen; Goat anti-Mouse IgG2a Fluor 647 3:400, Invitrogen; Goat anti-Mouse IgG2b Alexa Fluor 647 3:400, Invitrogen; Goat anti-Chicken IgY Alexa Fluor 647 3:400, Invitrogen) were diluted in 5% NDS or 5%NGS and left to incubate overnight at room temperature. Primary omissions were prepared the same way but without incubation in primary antibody. Successful observed labelling was not due to non-specific secondary antibody interactions since primary omission results showed lack of specific staining. Sections were then washed in PBST at room temperature for 1, 5, 10, and 60 minutes. Sections were then incubated in a 1:1000 dilution of DAPI and then washed in PBS at room temperature for 1, 5, and 10 minutes. Sections were then mounted in 90% glycerol and sealed with clear nail polish for confocal imaging.

Thin section imaging.

A Zeiss Laser Scanning Microscope 800 was used for imaging. The 10x water objective was used to visualize staining. The 647nm laser was used to image all samples with a gain of 520V, laser power of 2.5%, and pinhole of 100um. A single tile (765x765 pixel section) from the top of each cortex was imaged with the 25x water objective to observe antibody staining. Antibody staining efficacy was determined by comparing staining patterns to In Situ Hybridization images from the Allen Brain Atlas[21].

Thick tissue preparation- "The Cuboid Method".

Fixed and dehydrated brains were placed in a coronal matrix and cut into 2mm thick sections. Sections were then placed in a petri dish and cut into eight roughly 2mmx2mm pieces, referred to as “cuboids”. The cuboid method is depicted in the figure below. Cuboids are cut in this way to allow for right/left anatomical comparisons within one section of one brain.

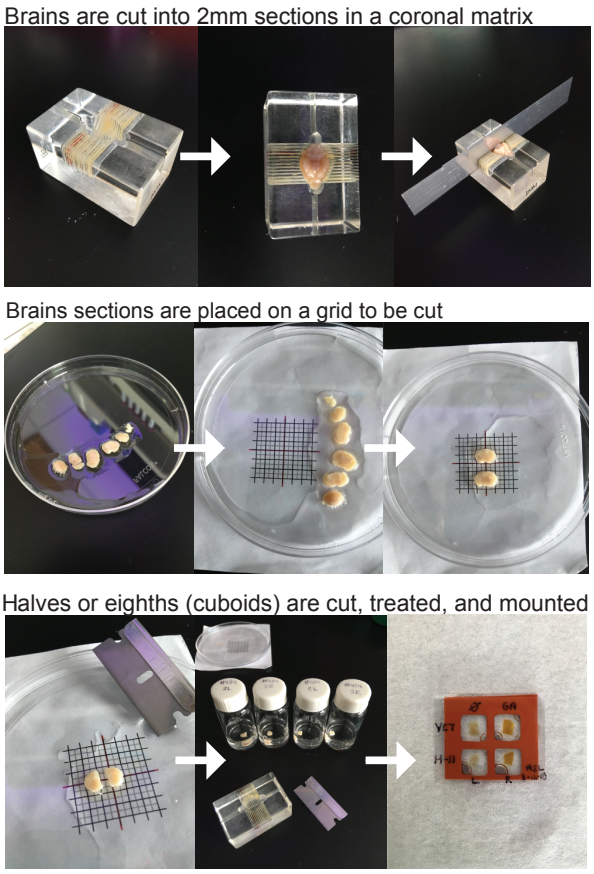

Figure 1 | “The Cuboid Method” – The above image depicts the process of cutting each brain into sections in the matrix and then cutting each section into further halves or eighths (cuboids) that are paired and subjected to different reagent conditions before mounting in a gasket and imaging.

Basic thick tissue fixation and immunohistochemistry.

Cuboids were placed in labelled 5mL tubes and fixed in 0.01% Glutaraldehyde at 4°C overnight. The cuboids were washed three times for five minutes in PBST and then quenched with 0.5mol/L Glycine overnight at 4°C to stop further glutaraldehyde cross-linking reactions. Cuboids were then washed three times for five minutes in PBST and cleared in 6% sodium dodecyl sulfate (SDS) for five days at 37°C. Cuboids were then washed for 2 days in PBST. Primary antibody (Chicken anti-SST 1:200, SYSY; Rat anti-SST 1:200, Millipore; Mouse anti-SST (H-11) 3:400, Santa Cruz Biotechnology Inc.; Rat anti-SST (YC7) 3:400, Santa Cruz Biotechnology Inc.; Mouse anti-SST (D-12) 3:400, Santa Cruz Biotechnology Inc.; Mouse anti-VIP (H-6) 3:400, Santa Cruz Biotechnology Inc.; Mouse anti-SST (G-10) 3:400, Santa Cruz Biotechnology Inc.; Goat anti-Parvalbumin 1:200, Abcam; Rabbit anti-Parvalbumin 1:200, GenScript; Rabbit anti-VIP 1:200, ImmunoStar) was then diluted in PBST, added to the cuboids and incubated for three days at 37°C. Primary antibody was then removed and cuboids were washed 3 times for three minutes and then left to wash for two days in PBST. Secondary antibody (Donkey anti-Rat Alexa Fluor 647 3:250, Invitrogen; Goat anti-Mouse IgG1 Fluor 647 3:250, Invitrogen; Goat anti-Mouse IgG2a Fluor 647 3:250, Invitrogen; Goat anti-Mouse IgG2b Alexa Fluor 647 3:250, Invitrogen; Goat anti-Chicken IgY Alexa Fluor 647 1:100, Invitrogen, Donkey anti-Rabbit Alexa Fluor 647 1:100, Invitrogen) was then diluted in PBST and added to cuboids to incubate for three days at 37°C. Secondary antibody was then removed and cuboids were washed three times for three minutes and then left to wash for two days in PBST. Primary omissions were also prepared in which the same steps as described were completed except for addition of primary antibody. Successful observed labelling was not due to non-specific secondary antibody interactions since primary omission results showed lack of specific staining Pieces were then placed in Iodixanol for refractive index matching and then mounted in Iodixanol in 2mm thick gaskets.

Variation to thick tissue preparation.

The above protocol was modified in several experiments to test effects of variables that differ between thick tissue and thin tissue staining. Glutaraldehyde (GA), Glycine, SDS, and blocking were omitted individually in different experiments, keeping the rest of the protocol constant.

Microscopy.

A ZEISS Confocal Laser Scanning Microscope 800 was used for imaging. The 10x water objective was used to image the cuboids. The 647nm laser was used to image PV staining in Glutaraldehyde and SDS treated tissue with a gain of 500v, laser of 0.5%, and pinhole of 76um. The 647nm laser was used to image SST staining in non-GA and non-SDS treated tissue with a gain of 520v, laser of 1.5%, and pinhole of 100um. Single tiles from the cortex were compared across samples for presence of antibody staining and Z-stacks were obtained to determine depth of antibody staining and effects of different reagents.

Image Display.

Experimental groups were imaged with the same laser, gain, and pinhole settings. Gamma was adjusted to the same value in all images to enable fair comparison of cell body brightness to background signal across samples. Z-stacks were made into orthogonal projections using Zen Image Processing Software.

Data Analysis.

ImageJ was used to count cells and Imaris was used to quantify the intensity of stained cells. Cells were counted in ImageJ by changing the image to greyscale (8bit), the adjusting the threshold to 1-2%, and analyzing particles that are 0.001-infinity inch^2, circularity 0.00-1.0. Cells in Imaris were chosen based on size, quality, and distance from the surface. Cell diameter across the x-y axis was chosen to have a 10μm minimum while diameter in the Z direction was chosen to have an 18μm minimum due to image distortion from confocal imaging. Background subtraction was used to smooth the surface and make it easier to determine foreground cells from background. Imaris data was processed by a custom program in MATLAB written by Dave Bulkin to determine foreground intensity, background intensity, and overall intensity for each Z layer. Results were then graphed in Excel.

Results

Testing SST, PV, and VIP antibody efficacy

To molecularly characterize GABA interneurons in thick tissue, antibodies targeted to three GABA interneuron subtypes, SST, PV, and VIP, were tested in thick tissue. Antibodies were selected based on successful results in thin tissue from a variety of sources[5,22,23]. Initially, SST, PV, and VIP antibodies were tested in 2mm thick tissue that was fixed for five days in 4%PFA with subsequent fixation in GA for 24 hours. Strong fixations are commonly used in thick tissue preparation to maintain tissue structure and integrity during clearing[15,17,24], thus thick tissue

prepared in a typical manner was used for initial antibody testing in thick tissue. All SST antibodies (Mouse anti-SST (H-11), Mouse anti-SST (D-12), Rat anti-SST (YC7), Mouse anti-SST (G-10), Millipore Mouse anti-SST, and Chicken anti-SST) and one VIP antibody (Mouse anti-VIP (H-6)) failed to stain neurons specifically in thick tissue. Both PV antibodies (Goat anti-PV and Rabbit anti-PV) and one of the VIP antibodies (Rabbit anti-VIP) did show specific labelling of neurons in thick tissue. Antibodies that failed to stain were tested further in an attempt to optimize them for thick tissue staining.

Thin tissue staining was conducted to determine whether the lack of staining with the six SST antibodies and one VIP antibody was due to incompatible thick tissue prep or ineffectiveness of the antibody itself. Results from staining 50μm thin tissue with each of the previously unsuccessful antibodies showed that Mouse anti-SST (H-11), Mouse anti-SST (D-12), and Rat anti-SST (YC7) were effective antibodies and worth pursuing in thick tissue (Fig. 1A). The three successful SST antibodies visibly stained cells, whereas Mouse anti-SST (G-10), Millipore Mouse anti-SST, Chicken anti-SST, and Mouse anti-VIP did not stain any cells even when imaged at 40x. This did not appear to be due to excessive background staining as all samples were imaged with the same gain and laser and failed samples did not appear brighter than successfully stained samples. Thus the lack of staining is attributed to failure of antibody to bind antigen, not excessive background. To count cells, single anatomically matched tiles from the cortex as shown in Fig. 1A were imaged with the same laser and gain to allow for fair comparisons between antibodies. Cells were detected and counted in ImageJ (Fig. 1B). The anti-SST (H-11) antibody stained the most cells, Rat anti-SST (YC7) stained the second largest number of cells, and Mouse anti-SST (D-12) stained the least number of cells (Fig. 1B). The successful thin tissue staining with the three SST antibodies

that had previously failed in thick tissue indicated that a component of the thick tissue preparation might be impacting epitope recognition.

A

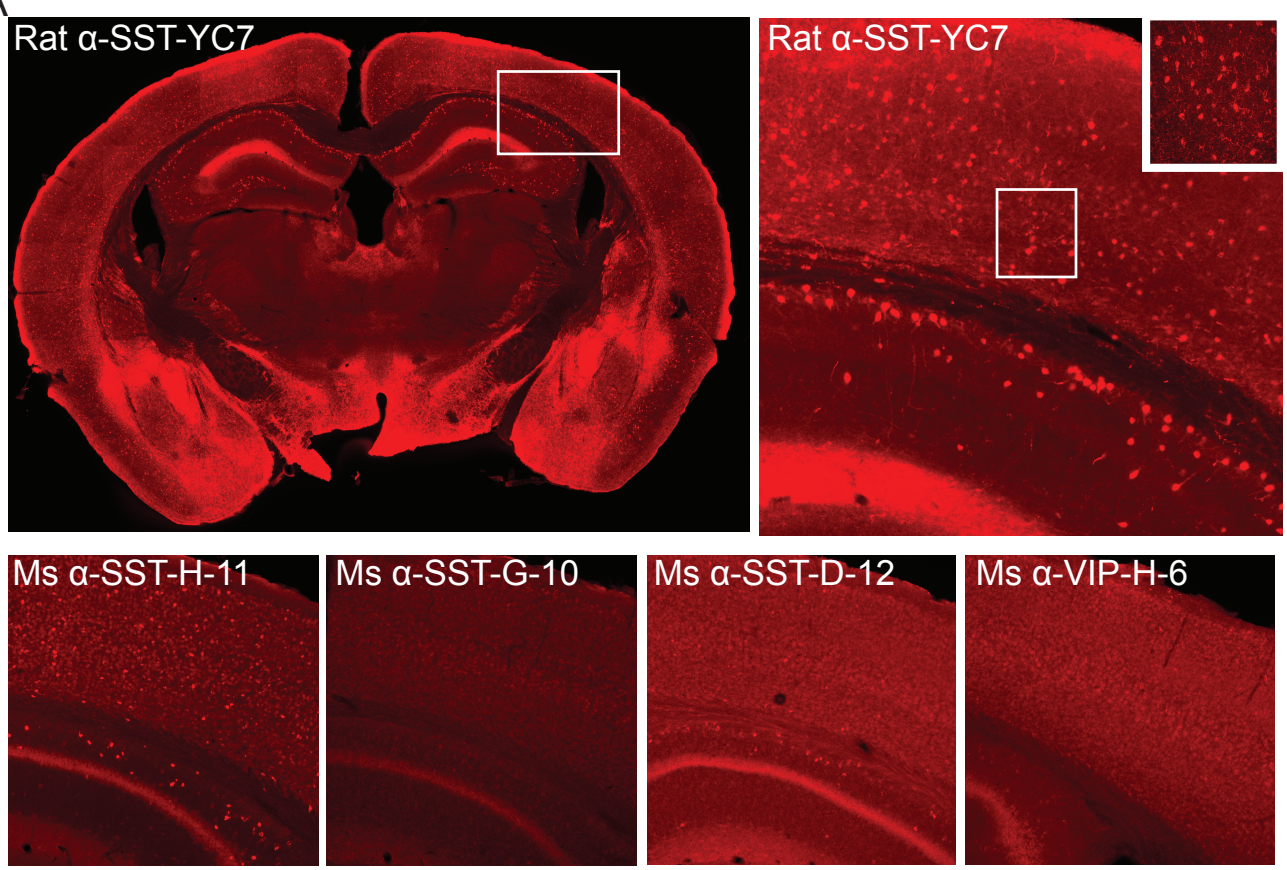
Rat α-SST-YC7
Rat α-SST-YC7
Ms α-SST-H-11
Ms α-SST-G-10
Ms α-SST-D-12
Ms α-VIP-H-6

B

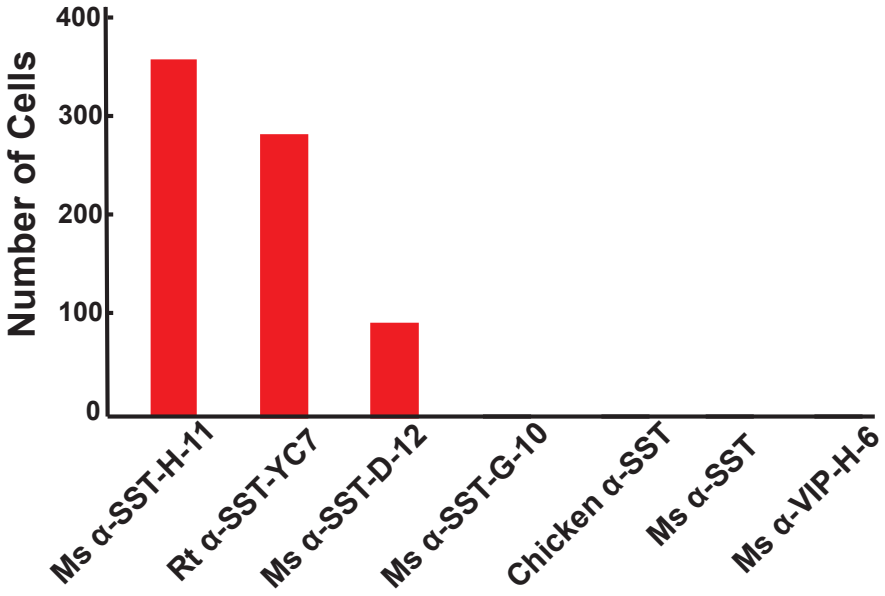
Number of Cells
400
300
200
100
0
Ms α-SST-H-11
Rt α-SST-YC7
Ms α-SST-D-12
Ms α-SST-G-10
Chicken α-SST
Ms α-SST
Ms α-VIP-H-6

Figure 2 -Thin tissue staining proves efficacy of three SST antibodies | **A,** Images showing SST and VIP antibody staining in thin sections. Staining was observed with Rat α-SST-YC7, Ms α-SST-H-11, and Ms α-SST-D-12. White box shown in the upper left image is the tile displayed in the upper right image. The white box in the middle of the upper right image depicts the area that was imaged at 40x to produce the small image in the corner of the upper right image. **B,** Bar chart showing number of cells counted in ImageJ for each antibody tested in thin section.

Thick tissue optimization for SST antibodies

Next, I looked at the factors that differ between the thin and thick tissue preparation and immunohistochemistry (IHC) in order to figure out what was preventing specific staining in thick tissue. In thick tissue preparation, there are multiple steps that differ from thin tissue preparation such as fixation with GA, quenching with glycine, delipidation with SDS, lack of blocking, refractive index matching in Iodixanol, and generally longer incubation periods and washes (Fig. 3). Major variables that impact staining such as fixation, blocking, and SDS treatment were tested independently to determine what might be preventing staining in thick tissue. To expedite the process of testing and to decrease costs of the thick tissue staining process, the cuboid method (described above in methods) was used. Using small cuboids of thick tissue minimizes reagent volumes as well as time needed for diffusion of both antibodies and wash solution. Despite the increased efficiency of this method compared to whole section or whole brain staining, the process still takes about 18 days from the moment of brain harvest to imaging the samples (Fig. 3).

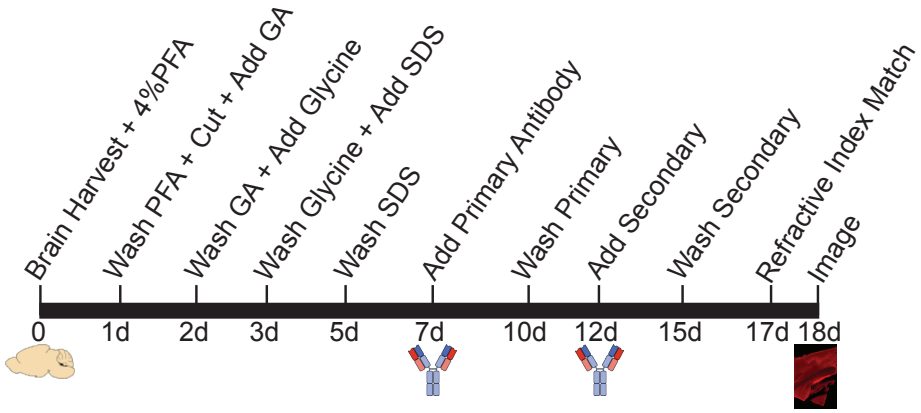

Figure 3 | Timeline depicting the process of preparing and staining thick tissue cuboids. This process was modified throughout experimentation to test effects of different variables on thick tissue IHC.

Mouse anti-SST (H-11), Mouse anti-SST (D-12), and Rat anti-SST (YC7), were chosen to test factors that affect staining. The timeline depicted in Figure 3 shows the baseline procedure that was used to prepare and stain thick tissue. Small variations to the timeline allowed testing of different factors affecting thick tissue staining while maintaining within-study control between experiments.

Duration of formaldehyde fixation

I first focused on testing a major factor that differed between thin and thick tissue preparation which was duration and type of fixation. The first aspect of fixation that I looked at was duration of fixation in 4%PFA. The brains that had been previously used for thick tissue experiments in the initial stages of the project had been drop fixed for five days in 4%PFA at 4°C. The SST antibodies were successful in thin sections drop fixed for only 24 hours in 4%PFA, so I tried staining thick tissue cuboids that had been subject to the following conditions: drop fix for 24 hours in 4%PFA

and drop fix plus SDS addition for 3 days. Minimal drop fix proved to be compatible with SST antibody staining in thick tissue for all three SST antibodies as did drop fix with SDS treatment (Fig. 4).

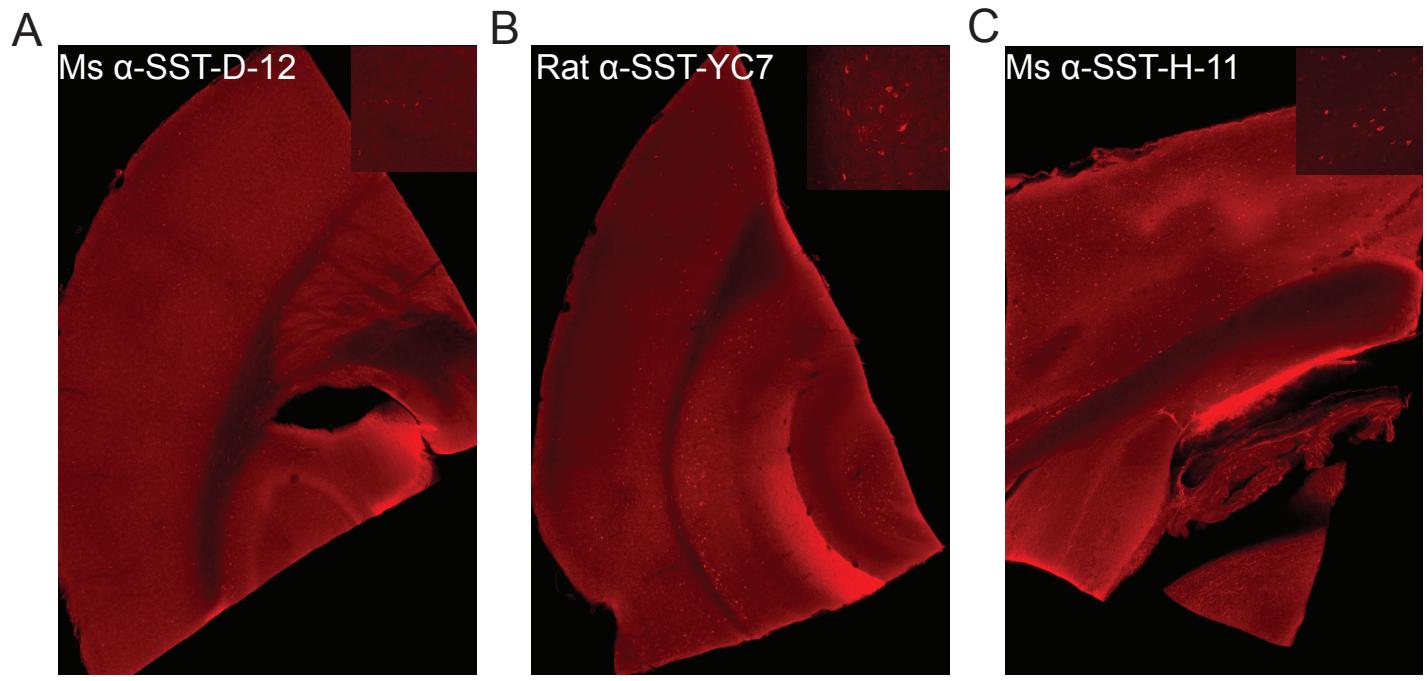

Figure 4 – SST Staining in lightly fixed, non-SDS treated, thick tissue |
Immunohistochemical staining of SST neurons in cuboid from the mouse cortex. Upper right hand panel shows 25x imaging of stained SST neurons. All cuboids were drop fixed in 4%PFA overnight and then stained as per the timeline in Figure 3. **A,** Immunohistochemical staining of SST neurons with Mouse anti-SST-D-12 antibody. **B,** Immunohistochemical staining of SST neurons with Rat anti-SST-YC7 antibody. **C,** Immunohistochemical staining of SST neurons with Mouse anti-SST-H-11 antibody.

Glutaraldehyde fixation

The next fixative tested was GA. GA is a very strong and fast working fixative[25] such that the maximum duration of GA fixation for thick tissue was 24 hours. Cuboids were drop fixed with 4% PFA for 24 hours and then treated with 10ul of 10% GA or drop fixed, treated with SDS and then treated with GA. The GA dose that was added was about 2-5x higher than typical protocols[15,17] in order to determine the impact that GA had on tissue staining. Both fixation experiments resulted in no specific neuronal staining with any of the SST antibodies and GA greatly increased surface auto-fluorescence compared to non-GA treated cuboids such that imaging with the same laser power as non-GA treated tissue led to saturation (Fig 5A). Figure 5A shows two anatomically matched cuboids from the same cortical brain slice. The only difference in treatment between the two cuboids was that the left was not treated with GA while the right one was treated with GA. The striatum and hippocampus are barely discernable in the GA overdosed cuboid compared to the non-GA treated cuboid. In addition, it is evident that there is antibody staining in the non-GA treated cuboid and no antibody staining detectable in the GA treated cuboid. Figures 5B and 5C show the impacts GA can have on auto-fluorescence over depth. Images B and C were taken with the same laser power and gain and are depicted in range indicator, a LUT that makes the lowest signal black and the highest signal white, such that saturated fluorescence is white and no signal is black. It is evident that the GA treated cuboid has much higher fluorescence throughout the tissue in comparison to the non-GA treated cuboid. GA created very high auto-fluorescence on the surface of the tissue, indicated by the peak in the graph in Figure 5E. Both Figure 5D and 5E show that auto-fluorescence drops off significantly further into the tissue but never reaches signal levels as low as non-GA treated tissue. The drop off in auto-fluorescence intensity is much more evident throughout tissue depth in the GA treated chunk than in the non-GA treated chunk.

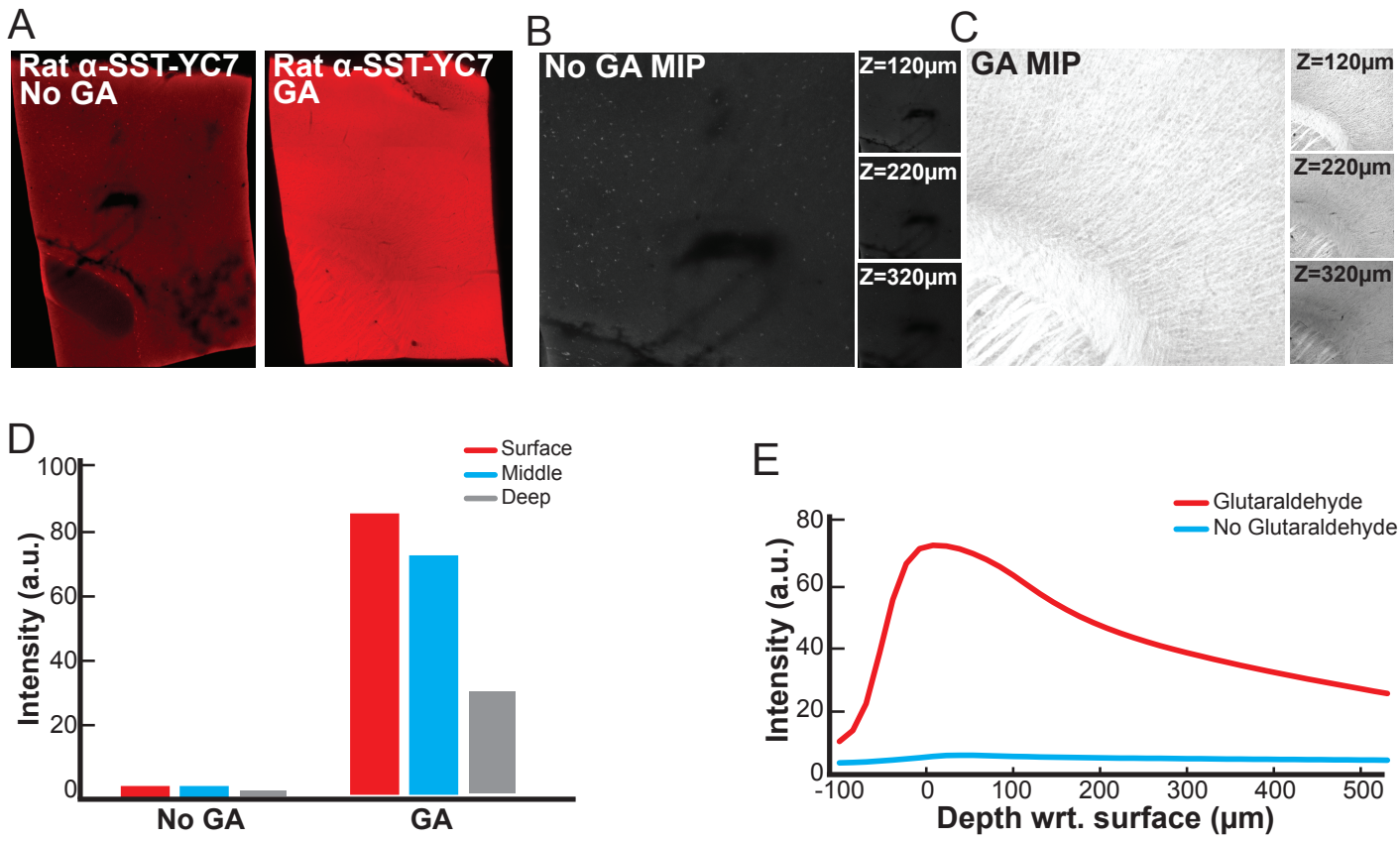

Figure 5 – Effects of glutaraldehyde on tissue staining and fluorescence| **A,** Left image is a cuboid dropped fixed for 24hr in 4%PFA and not treated with GA. Right image is an anatomically matched cuboid from the same brain section that was dropped fixed for 24hr in 4%PFA and treated with 10ul of 10% GA. Identical imaging settings were used when imaging the two cuboids. **B,** Large image is a maximum intensity projection of a single tile from non-GA treated cuboid in 5A displayed in range indicator. Smaller images are single plan Z-stacks depicting the change in fluorescence moving deeper into the tissue. **C,** Large image is a maximum intensity projection of a single tile from the GA treated cuboid in 5A displayed in range indicator. Smaller images are single plane Z-stacks depicting the change in fluorescence moving deeper into the tissue. **D,** Bar chart showing average signal intensity throughout depth in the non-GA and GA treated cuboids from 5A. Average signal intensity was calculated from single Z-stacks at the surface, in the

middle, and deep into the cuboids. **E,** Line graph showing the change in average signal intensity over depth for the non-GA and GA treated cuboids in 5A.

Effects of GA on SST vs PV immunohistochemistry

After seeing that high doses of GA dramatically increased the background when staining for SST, I tested the impacts of high doses of GA on PV staining with the Rabbit (Rab) anti-PV antibody. The exact same cuboid treated with 10ul of 10% GA that failed to stain with SST H-11 was stained with Rab anti-PV successfully. The within cuboid control increases confidence that SST and PV antibodies are impacted differently by GA fixation such that PV produces cell staining in over-fixed tissue, while SST antibodies do not stain over fixed tissue as shown in figure 6 A and B. The Z depth images in Figure 6 show that antibody staining with the PV antibody is much more effective on the surface than throughout the tissue when over fixed with GA.

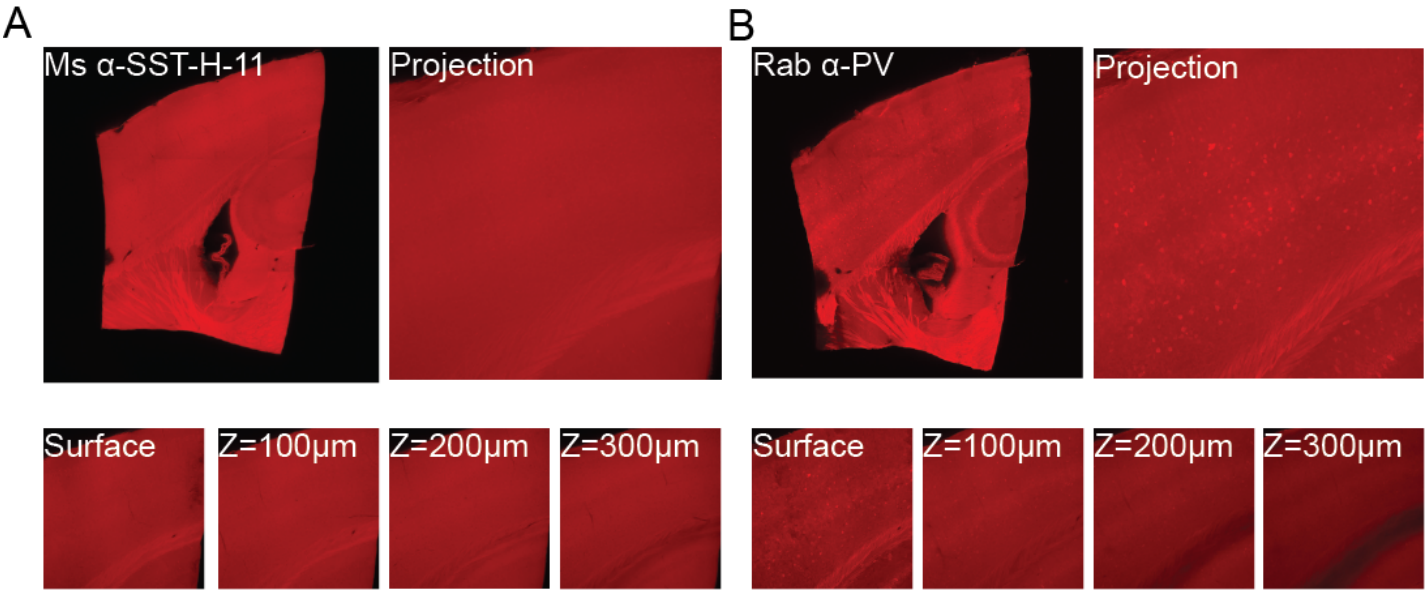

Figure 6 – Glutaraldehyde impacts PV and SST staining differently | **A,** Upper left image depicts GA treated cuboid stained with Mouse anti-SST-H-11. Upper right image shows a maximum intensity projection of a single tile of cortex. No staining is evident. Lower images are

single Z layers at the surface, 100μm, 200μm, and 300μm into the tissue. **B,** Same as in **A** except cuboids were treated with Rab anti-PV and staining was evident.

Effects of post SDS treatment on staining

SDS treatment is commonly used to clear lipids from tissue to enhance deeper imaging in thick tissue[26,27], and also to enhance antibody penetration depth. I was interested in observing the effects of SDS treatment after immunohistochemical staining with SST. SDS has been shown to denature proteins and prevent epitope recognition[27], thus making it possibly beneficial to perform IHC prior to delipidation to enhance epitope recognition. On the contrary, SDS has also been shown to remove antibody staining at both high temperatures[17] and low pH[28], thus possibly making it counter-productive to stain and then delipidate tissue. Not only has SDS been shown to remove staining, but also decrease fluorescence by denaturing fluorphores[27,28]. I wanted to see if SDS treatment at a mild pH and 37°C could delipidate cuboids without removing antibody or denaturing epitopes and fluorophores. Cuboids treated with only 4%PFA were incubated in primary antibody against SST and then compatible secondary antibody. Cuboids were imaged to determine baseline staining (Fig 7). Cuboids were then dismounted, washed, and treated with 2% SDS for 2 days at 37°C. Cuboids were then imaged again to determine the intensity of antibody staining post SDS treatment. As shown in Figure 7, antibody staining intensity and background signal both decreased for all three antibodies. Mouse anti-SST D-12 showed the most drastic decrease in SST signal, with only two cells still visible after SDS treatment (Fig. 7B). The cuboids were then again dismounted, washed, and incubated in secondary antibody to determine if the decrease in signal after SDS was due to denaturing the fluorophore or if it was due to denaturing or removal of primary antibody. I expected that denaturing the fluorophore was responsible for decreased signal

but surprisingly, adding secondary antibody did not increase antibody specific SST signal (Figure 7). The background signal appeared to increase but the number of visibly stained cells did not increase from post SDS levels. Figure 7B shows that cell number continued to decrease after secondary antibody addition. The continued decrease in cell bodies could be due to extra washing or too much time spent at 37°C. Images in Figure 7 are all maximum intensity projections that range from Z levels at the surface to a Z level of 400µm. Images are displayed in range indicator to show increases and decreases in background and foreground signal intensity.

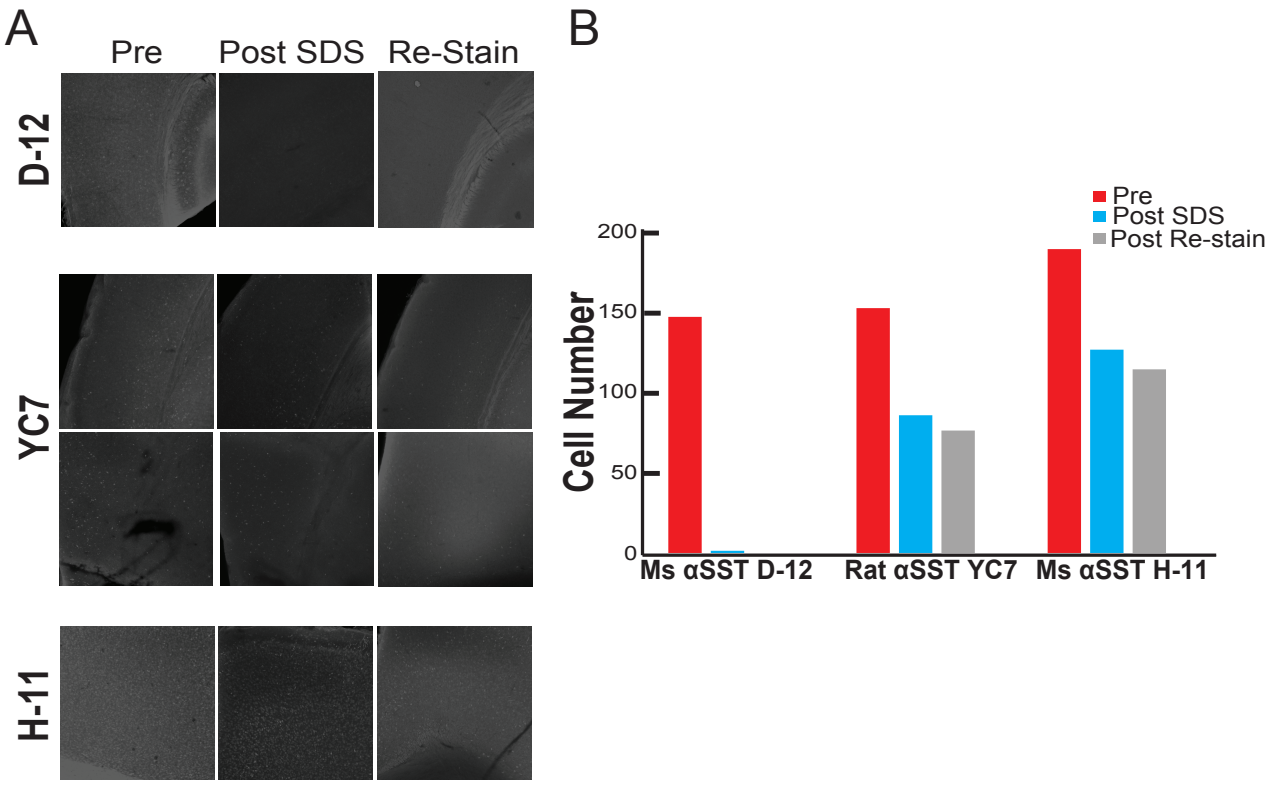

Figure 7 – Impacts of post-staining SDS treatment | **A,** Images showing single tile maximum intensity projections of cuboids stained with all three successful SST antibodies. Stages of experiment are depicted across the top. Leftmost images showing SST staining in 4%PFA treated cuboids across all three antibodies. The middle images show staining in the same cuboids after

SDS treatment. The rightmost images show the same cuboids after being re-stained with secondary antibody. All images are displayed in range indicator to best show changes in signal intensity. **B,** Bar chart showing the change in number of detectable stained cells across all three antibodies. 'Pre' refers to cell bodies detected in normally stained tissue. 'Post SDS' refers to cell bodies detected after incubating the stained cuboids in SDS. 'Post Re-stain' refers to cell bodies detected after incubating the SDS treated tissue in secondary antibody. The two Rat anti-SST-YC7 trials were averaged to give average number of cells stained at each experimental stage. Decrease in cell number is evident across all antibodies.

Effects of blocking in thick tissue

Next, I tested whether blocking in thick tissue might enhance staining. Blocking is typically used in IHC protocols to minimize non-specific antibody binding and decrease high background[29,30]. Blocking was used in the thin tissue experiments in which SST neurons were successfully stained, thus I hypothesized that blocking in thick tissue might enhance staining to the level that was achieved in thin tissue. One pair of cuboids were drop fixed in 4% PFA, treated with SDS, and stained with Rabbit anti-PV, while the other pair was drop fixed, treated with GA, then treated with SDS, then stained with Mouse anti-SST H-11. One cuboid from each set was blocked for one hour prior to staining in either 10% NDS or 10% NGS (per methods section) depending on secondary antibody, while the other cuboid was not blocked. Primary and secondary incubations were both done in 5% blocking solution. Background fluorescence appeared to be similar between blocked and non-blocked tissue (Fig. 8A). The cuboids stained with Rab anti-PV showed significant cell body staining regardless of blocking (Fig. 8A). I expected there to be a much lower surface fluorescence for blocked tissue versus non-blocked tissue and that this difference in

fluorescence would become negligible by the middle of the tissue. There did not appear to be a major difference in tissue surface fluorescence intensity between blocked and non-blocked samples, in fact the blocked sample appeared to have slightly higher surface fluorescence than the non-blocked sample (Fig. 8B). Fluorescence intensity appeared to decrease at a similar rate in both cuboids, reaching a similar low level of fluorescence by 250μm into the tissue. In the GA treated cuboids stained with Mouse anti-SST H-11, there also did not appear to be a difference in average fluorescence intensity between the blocked and non-blocked cuboids (Fig. 8C). Cuboids both appeared to have minimal staining due to GA but blocking did not enhance staining since there did not appear to be more cell bodies nor better signal for stained cell bodies (Fig. 8C). The line graph in Figure 8D shows that in GA treated tissue, blocking does not decrease average fluorescence as initially expected. In fact, cuboids have very similar average surface fluorescence levels and at about 250μm average fluorescence in both cuboids reaches the same level (Fig. 8D).

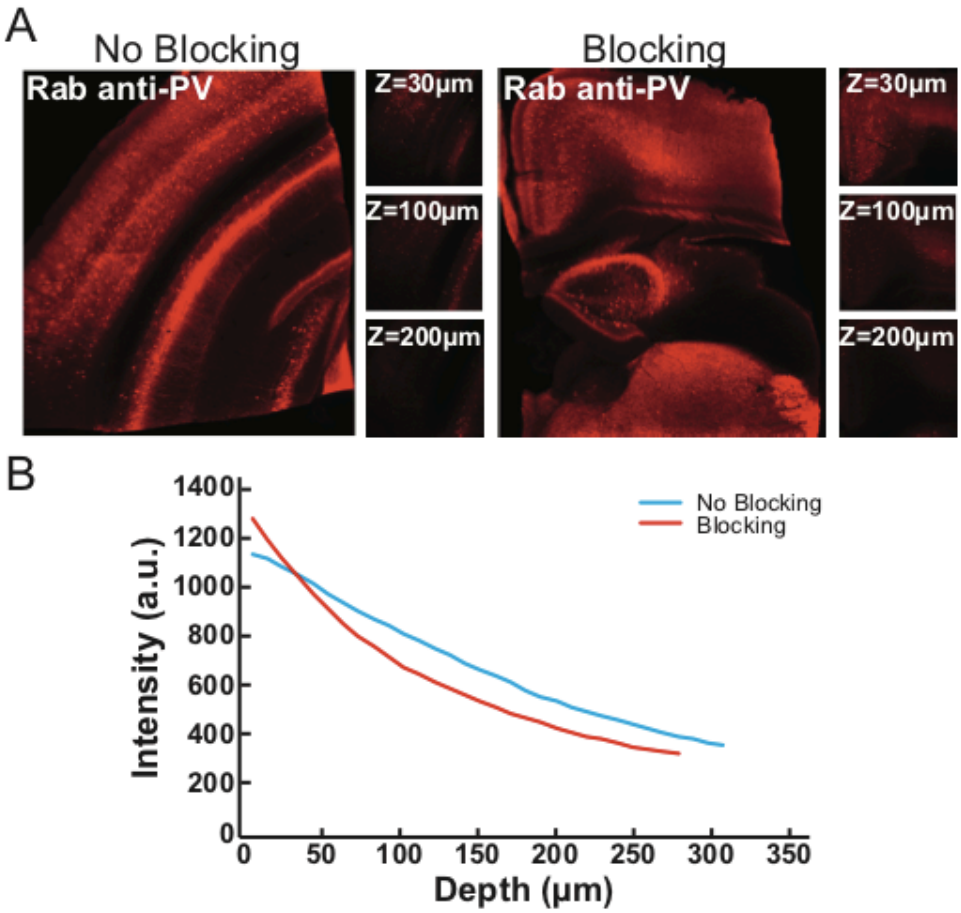
A
No Blocking
Blocking
Rab anti-PV
Rab anti-PV
Z=30μm
Z=100μm
Z=200μm
Z=30μm
Z=100μm
Z=200μm
B
Intensity (a.u.)
Depth (μm)
No Blocking
Blocking
0
200
400
600
800
1000
1200
1400
0
50
100
150
200
250
300
350

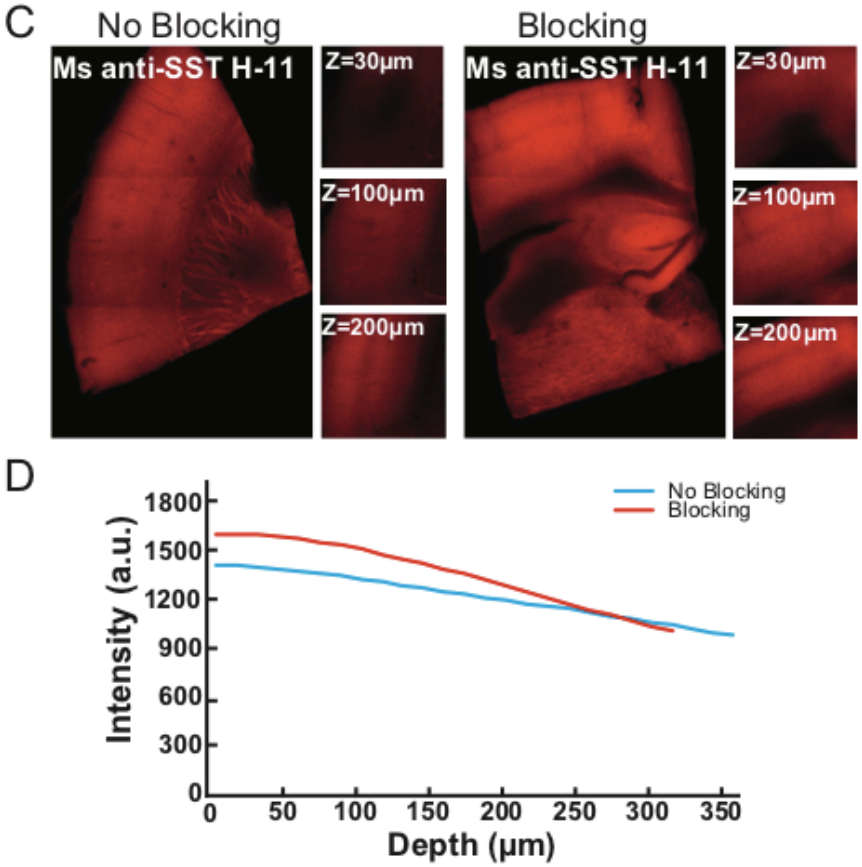

Figure 8 – Impact of blocking on background staining | **A,** Large images show effects of not blocking versus blocking in cuboids stained with Rab anti-PV. Smaller images show average intensity and staining at Z depths of 30µm, 100µm, and 200µm into the tissue. **B,** Line graph showing difference in average fluorescence intensity over depth in Rab anti-PV stained tissue between blocked and non-blocked tissue. **C,** Image showing effects of not blocking versus blocking in cuboids stained with Mouse anti-SST H-11 and treated with GA. Smaller images show average intensity and staining at Z depths of 30µm, 100µm , and 200µm into the tissue. **D,** Line graph showing difference in average fluorescence intensity over depth in Mouse anti-SST H-11 stained tissue between blocked and non-blocked tissue. Cell body counts from each maximum intensity projection were determined in ImageJ.

Antibody comparisons in thick tissue

All six successful GABA interneuron antibodies were evaluated based on cell count and average signal to noise ratio. Cuboids stained with SST antibodies (D-12, YC7, and H-11) and the Rab anti-VIP antibody were treated with 4%PFA overnight at 4°C as this treatment resulted in the best staining. Cuboids stained with Goat anti-PV and Rab anti-PV were treated with 4%PFA overnight, 0.5% GA overnight, and then treated with 6% SDS as these were the conditions initially tested in thick tissue that produced good results. Figure 8A shows 10x imaging of single tiles of each cuboid made into maximum intensity projections to show cell staining between the surface and 400μm deep. Figure 8B shows 25x imaging of successfully stained cells. Both images show the sparsity of SST and VIP staining compared to PV staining. Background staining appears to be highest for the VIP antibody. The graph in Figure 8C depicts signal to noise ratios for each antibody based on all Z stacks in the maximum intensity projections for each cuboid in 8A and 8B. The bar chart shows that the PV antibodies had the best signal to noise ratio, determined by dividing the signal of the cells by the signal of everything except the cells. The SST H-11 showed to have the best signal to noise ratio of the SST antibodies. The VIP antibody appeared to have the lowest signal to noise ratio, evident in Figure 8A and B as it is hard to determine cells from background fluorescence. From the graph in Fig. 8D it is evident that the PV antibodies stained the most cells, SST antibodies stained the second largest number of cells with SST H-11 staining the highest number of cells. The VIP antibody appeared to stain the least number of cells.

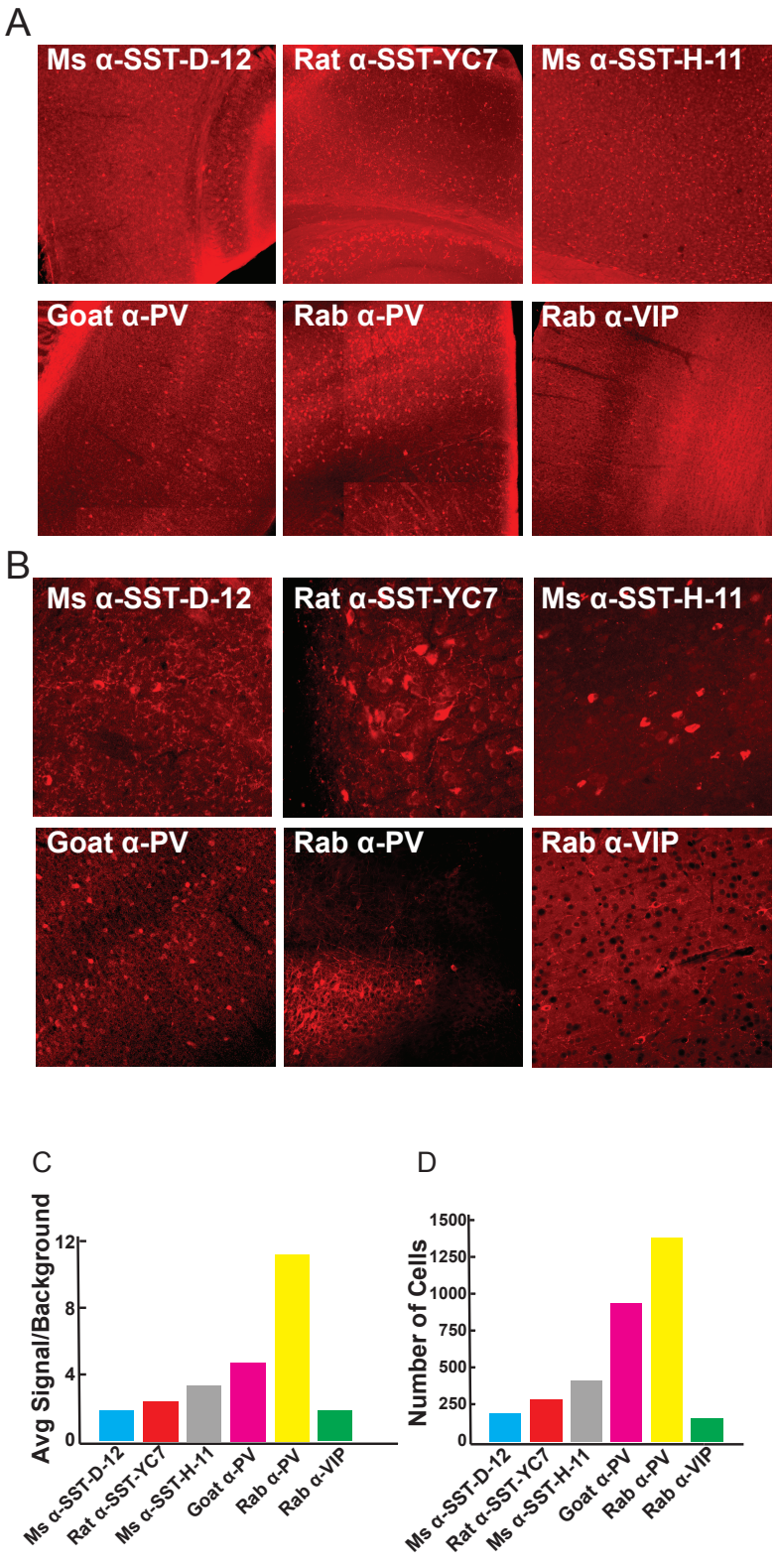

Figure 9 – Successful staining with SST, PV, and VIP antibodies | **A,** 10x imaging of all GABA interneuron antibodies that successfully stained thick tissue. All images are maximum intensity

projections of single tiles from PFC cuboids. **B,** 25x imaging of stained cell bodies from cuboids in 9A. **C,** Bar graph showing signal to background comparison across antibodies. Average signal of cell bodies was divided by average signal of everything else except cell bodies across all Z-depths to calculate ratios for all antibodies. **D,** Bar chart showing number of cells counted in ImageJ for each antibody. Cell counts were obtained from the maximum intensity projections in 9A, and thus represent a volume of XX x YY x ZZ μm.

Next, the three SST antibodies were further compared to determine differences in signal-noise ratios across Z-depths in the tissue. The signal to noise ratios for these antibodies were plotted over depth into the tissue to determine which antibody had the best staining deep into the tissue since the goal of the experiment is to successfully stain thick tissue with GABA interneuron antibodies. It is evident that Mouse anti-SST D-12 has by far the lowest signal to background ratio such that signal is only 1.5 times as intense as background fluorescence (Fig. 10). It is interesting that deep into the tissue the signal to background ratio improves by about 25% for the Rat anti-SST YC7 antibody such that deep into the tissue the H-11 and YC7 signal to background ratios reach similar levels (Fig 10). The graph shows that in general H-11 appears to have cell body signal that is 2.5 times the background signal. The YC7 antibody appears to have cell body signal 2 times that of the background at the surface. The YC7 signal to noise ratio increases deep into the tissue such that at 400μm the signal is about 2.4 times that of the background. The D-12 antibody appears to have the lowest cell body fluorescence at 1.5 times that of the background signal.

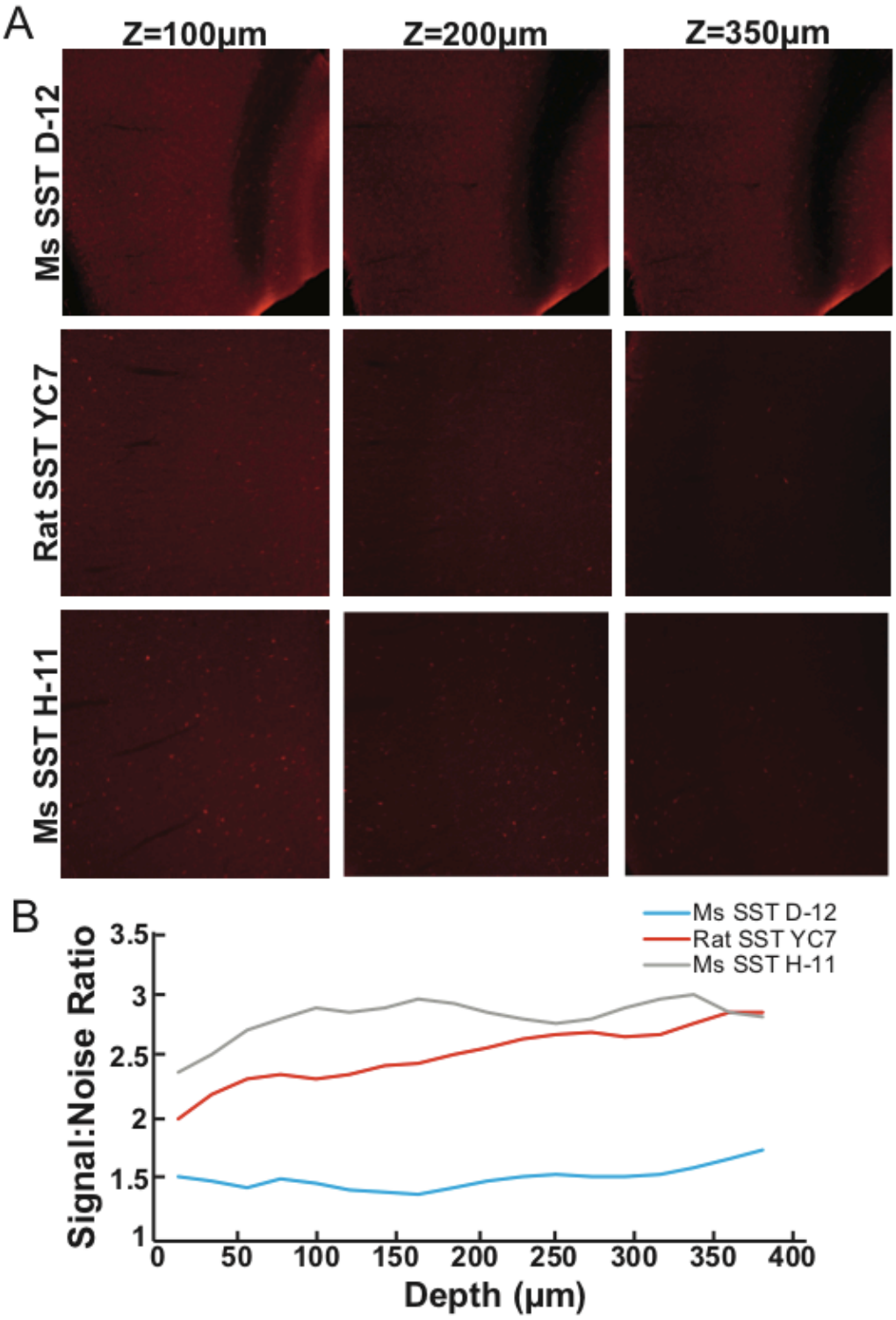

Figure 10 – Differential staining quality between three successful SST antibodies | **A,** Images showing staining across each successful SST antibody at Z depths of 100µm, 200µm, and 350µm.

B, Line graph showing the average signal to background ratio for each of the successful SST antibody throughout depth. Average cell body signal intensity from each Z layer in a single tile was divided by the average intensity of everything except the cell bodies in each Z layer to determine ratios at each depth.

Comparison of transgenic and IHC labelling of PV and SST neurons

Once immuno-staining with antibodies against each GABAergic subtype had been achieved, I was interested in looking at how similar IHC staining was to transgenic labelling of SST and GABAergic subtypes. To determine the accuracy of immunostaining within samples, PV-Cre mice expressing TdTom in PV neurons were used to look at the overlap of PV staining with transgenically labelled PV neurons and SST-Cre mice expressing TdTom is SST neurons were used to look at the overlap of SST staining with transgenically labelled SST positive neurons. Initially, PV-Cre mouse brains were dissected to look at the overlap between transgenic labelling of PV neurons and immunohistochemical labelling of PV neurons. Unfortunately, the PV-Cre line did not work as expected. TdTom was expressed in almost all neurons, not specifically in PV neurons when the expression pattern was compared to In Situ Hybridization (ISH) data of PV RNA from the Allen Brain Atlas[21]. Luckily, the SST-Cre mice had successful TdTom expression in SST neurons when compared to ISH data from the Allen Brain Atlas[21]. SST-Cre brains were stained with both PV and SST antibodies to look at population overlap. The 25x image in Figure 11A shows the two distinct PV and SST populations of GABAergic interneurons in the PFC. The Rab anti-PV antibody, depicted in cyan, stained a distinct subset of neurons from the SST neurons transgenically labelled with TdTom. The difference in staining is indicated by the cyan and magenta arrows in Figure 11. This corroborates data showing that these GABAergic subtypes of neurons represent distinct populations[31–33]. Overlap in SST staining and transgenic SST expression

was observed when SST-Cre brains were stained with Rat anti-SST YC7 antibody (Figure 11B). Transgenically labelled SST neurons, shown with magenta cell bodies, express TdTom driven by Cre. Magenta neurons appear to have peripheral staining around the cell body due to Rat anti-SST, shown in cyan. The 25x image in Figure 11B shows the overlap between transgenic and IHC labelled SST neurons in multiple cells. This confirms that the Rat anti-SST YC7 antibody is successful since it stained cells that transgenically express SST.

An internal study was also conducted in this experiment to look at the differences in morphology and staining of brain sections fixed with 3µl of 10% GA for 24hr versus not fixed with GA. Both Figure 11A and Figure 11B show thick brain sections with one side fixed in GA and the other side not fixed in GA. Below the full coronal images in both 11A and 11B, maximum intensity projections are shown depicting single cortical tiles from the GA fixed side and the non-GA fixed side. It appears that overall auto-fluorescence is brighter in the GA fixed sections than the non-GA fixed sections, as described above. The PV stained sections have similar staining patterns regardless of GA addition. The SST stained section appears have less staining when fixed with GA. Since the GA dose in this experiment was more moderate, at 3µl per half 2mm section, minimal SST staining was observed whereas cuboids fixed with 10µl of GA did not have any staining at all. The tissue appears somewhat more intact in GA treated sides since strong fixatives like GA are meant to preserve tissue structure.

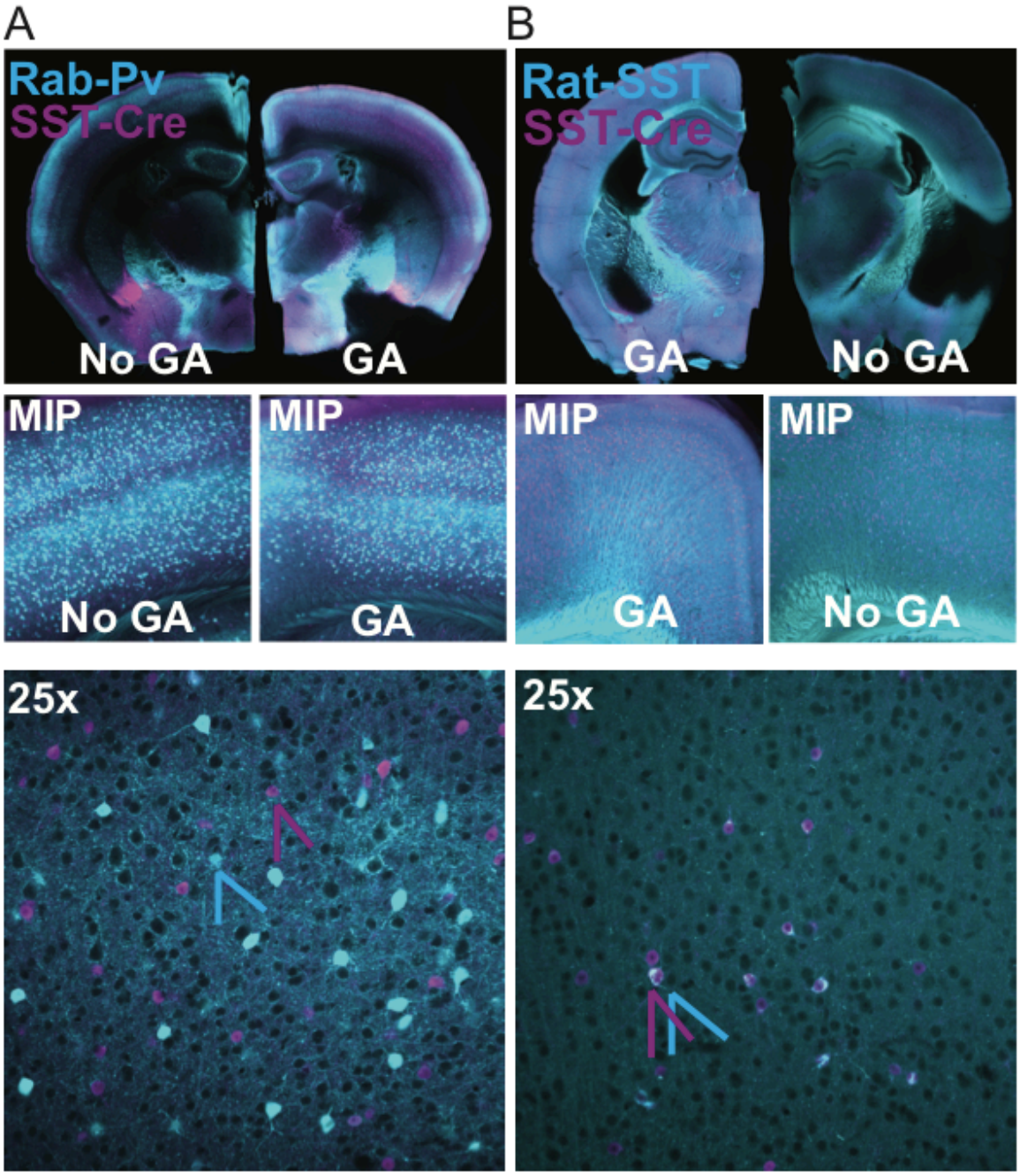

Figure 11 – Comparison of transgenic labelling with PV and SST staining in SST-Cre mice | **A,** Upper image is 2mm rostral section of transgenic SST-Cre-TdTom mouse brain stained with Rab anti-PV. TdTom expressing SST neurons are depicted in magenta while immunohistochemically labelled PV neurons are depicted in cyan. The left side of the Rab anti-PV stained brain was dropped fixed in 4%PFA for 24hr and then cleared with 1% SDS while the

right side was dropped fixed in 4%PFA for 24hr, fixed in 3µl of 10% GA for 24hr, and then cleared with 6% SDS.. The four middle images are maximum intensity projections of single cortical tiles from each brain section half. The lower 25x image shows no overlap between PV and SST populations in non-GA treated brain. **B,** Same as **A** but brain section is stained with Rat anti-SST YC7. The left side of the SST stained brain was dropped fixed in 4%PFA for 24hr, fixed in 3µl of 10% GA for 24hr, and then cleared with 6% SDS while the right side was dropped fixed in 4%PFA for 24hr and then cleared with 1% SDS. The lower 25x image shows overlap between transgenic SST and IHC labelled SST in non-GA treated brain.

Double staining with PV and SST antibodies

It is important to be able to stain for multiple GABAergic subtypes in the same tissue since this molecular characterization will allow for future experiments to interpret relative activity of subtypes during behavior. Thus, tissue was prepared in such a way to allow for both SST and PV staining to show that staining for at least two GABAergic subtypes simultaneously in thick tissue is possible. Mouse anti-SST H-11 and Rabbit anti-PV were used to double stain in one cuboid while Rat anti-SST YC7 and Rabbit anti-PV were used to double stain in another cuboid. VIP was not used since it was also raised in Rabbit and this would cause both PV and VIP neurons to be stained indiscriminately. Cuboids were drop fixed for 24 hours in 4%PFA and then delipidated in SDS and then stained with both antibodies simultaneously. Figure 12 shows the successful double staining with SST neurons labelled in magenta and PV neurons labelled in green. It is evident that there are more PV neurons stained than SST neurons in both cuboids. This finding is consistent with the cell counting results in Figure 9 showing that there are more PV neurons than SST neurons in the mouse PFC. The lack of overlap between the two GABAergic subpopulations is evident in

Figure 12 in the 25x imaging which is consistent with transgenic versus IHC results from the Figure 11 in which PV staining did not overlap with transgenic expression of SST. One observation that was noted with SST antibodies is that the fibrous tracts in the striatum appear to stain quite intensely as noted in the upper right image of Figure 10.

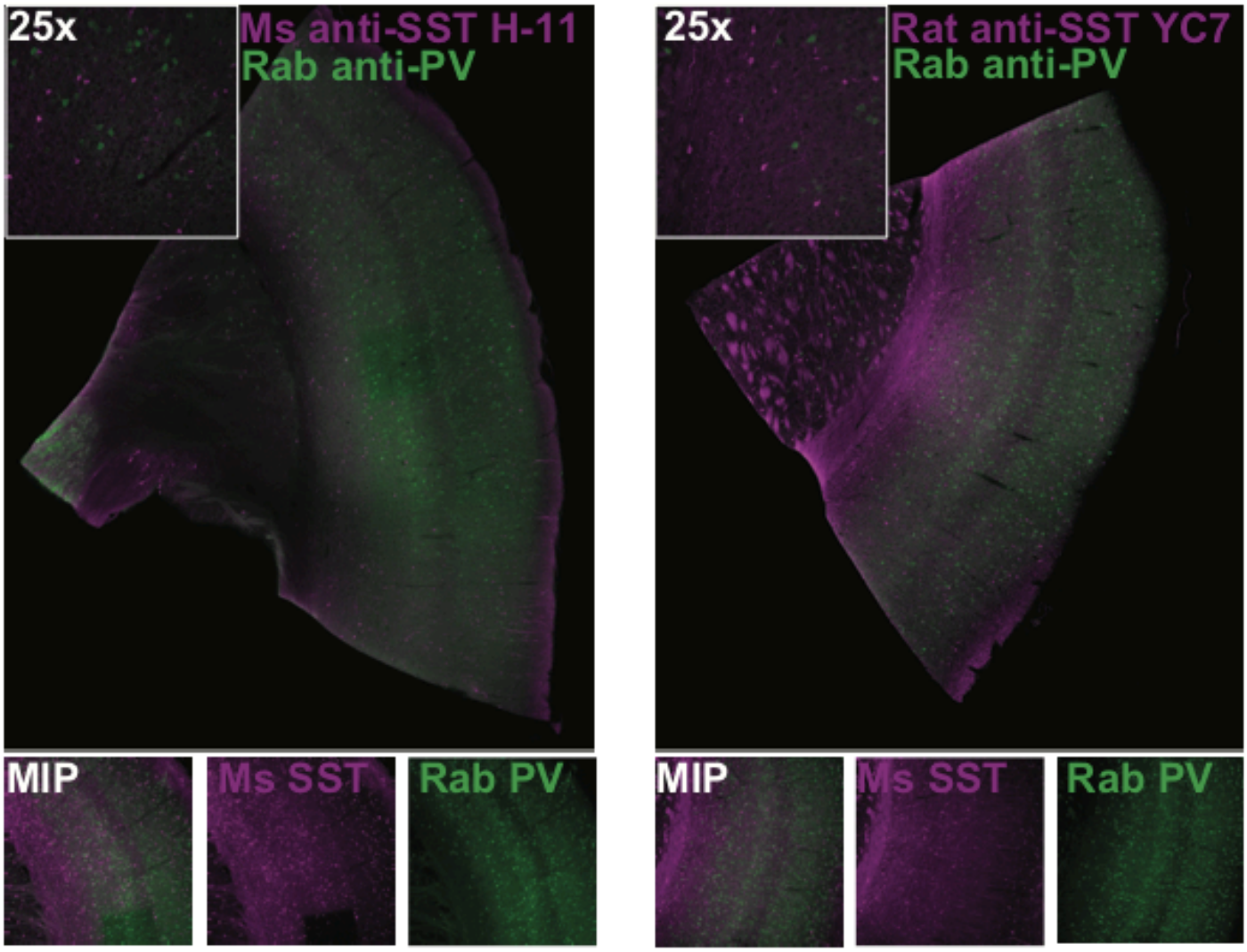

Figure 12 – Successful double labelling with SST and PV in mouse PFC | Images showing successful double staining with Mouse anti-SST H-11 and Rabbit anti-PV and also with Rat anti-SST YC7 and Rabbit anti-PV. Cuboids were fixed in 4%PFA for 24 hours and then treated with 2% SDS for 2 days and then stained with the respective antibodies. Smaller 25x images show lack

of overlap between populations of SST and VIP. Bottom images show the maximum intensity projections of a single tile with both individual channels depicted side by side to show staining in both channels.

Primary Omissions

Primary omissions were conducted for each secondary antibody used in the final results to show the background signal and autofluorescence of the tissue without primary antibody labelling. Low background was observed showing that specific staining was due to primary antibody interactions. It is evident that with the Gt a-MsIgG1 the striatum appears stained with secondary. This was observed in a few samples using this secondary thus this pattern was determined to not be due to specific staining of SST.

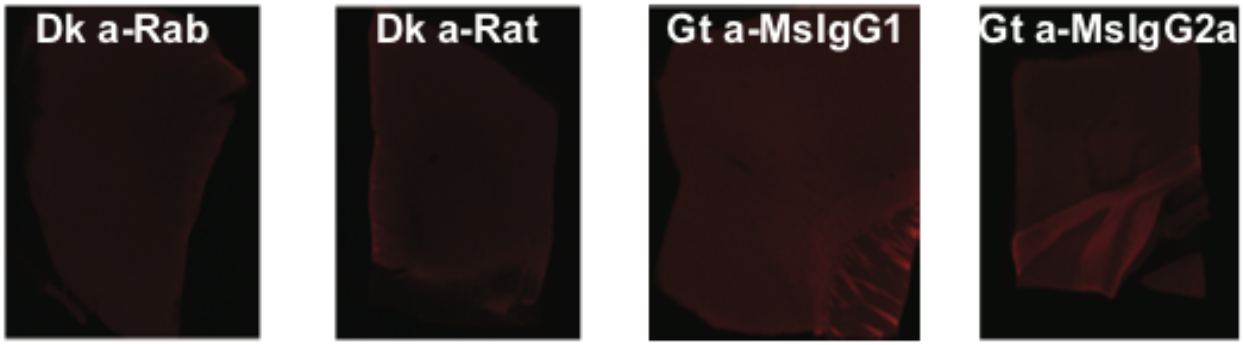

Figure 13 – Primary Omissions | Images showing background signal and tissue autofluorescence of four secondary antibodies used in SST, PV, and VIP immunostaining.

Antibody testing

The following charts summarize the GABA interneuron antibodies that were tested. Antibodies were selected based on literature showing successful staining results in thin tissue.

Primary Antibody	Host	Clonality	Amount and Concentration	Dilution Factor	Company	Catalogue Number	Staining in thick tissue	Rating in thick tissue (1-5)
anti-Somatostatin	Chicken	polyclonal	5ul of unavailable concentration	1:200	SYSY	366 006	no	-
anti-Somatostatin	Rat	polyclonal	5uL of 1mg/ml	1:200	Millipore	MAB354	no	-
anti-Somatostatin (H-11)	mouse	monoclonal	7.5uL of 0.2mg/ml	3:400	Santa Cruz Biotechnology Inc.	sc-74556	yes	5
anti-Somatostatin (YC7)	Rat	monoclonal	7.5uL of 0.2mg/ml	3:400	Santa Cruz Biotechnology Inc.	sc-47706	yes	5
anti-Somatostatin (D-12)	Mouse	monoclonal	7.5uL of 0.2mg/ml	3:400	Santa Cruz Biotechnology Inc	sc-25262	yes	3
anti-Somatostatin (G-10)	Mouse	monoclonal	7.5uL of 0.2mg/ml	3:400	Santa Cruz Biotechnology Inc.	sc-55565	no	-
anti-Parvalbumin	Goat	polyclonal	5uL of 0.5mg/mL	1:200	Abcam	ab32895	yes	3
anti-Parvalbumin	Rabbit	polyclonal	5uL of 0.5mg/mL	1:200	GenScript	A01439-40	yes	5
anti-Parvalbumin	Rabbit	polyclonal	7.5uL of 1ug/uL	1:200	Bioss	bs-1299R	no	-
anti-Vasoactive Intestinal Peptide	Rabbit	polyclonal	7.5uL unavailable concentration	1:200	ImmunoStar	20077	yes	3
anti-Vasoactive Intestinal Peptide (H-6)	Mouse	monoclonal	7.5uL of 0.2mg/ml	3:400	Santa Cruz Biotechnology Inc.	sc-25347	no	-

Table 1. Primary antibodies tested against SST, PV, and VIP. Antibodies were used to stain cortical mouse GABA interneurons in 2mm thick tissue. The rating reflects the overall ability of the antibody to stain thick tissue in addition to the number of cells stained and intensity of cell body staining.

Secondary Antibody	Host	Conjugated Fluorophore/Dye	Concentration	Dilution Factor	Company	Catalogue Number
anti-Chicken IgY (H+L)	Goat	Alexa Fluor 647	10uL of 1mg/ml	1:200	Invitrogen	A-21449
anti-Rat IgG (H+L)	Donkey	Alexa Fluor 647	12uL of 1mg/mL	1:200	Invitrogen	A-31573
anti-Mouse IgG1	Goat	Alexa Fluor 647	12uL of 0.5mg/ml	3:400	Invitrogen	A21120
anti-Mouse IgG2b	Goat	Alexa Fluor 647	12uL of 0.5mg/ml	3:400	Invitrogen	A21140
anti-Mouse IgG2a	Goat	Alex Fluor 647	12uL of 0.5mg/ml	3:400	Invitrogen	A21130
anti-Goat IgG (H+L)	Donkey	Alexa Fluor 633	10uL of 1mg/mL	1:200	Invitrogen	A21447
anti-Rabbit IgG (H+L)	Donkey	Alexa Fluor 647	10uL of 1mg/ml	1:200	Invitrogen	A31573

Table 2. List of all secondary antibodies tested. Concentration and volume of SST secondary antibodies was determined by multiplying successful volumes from thin tissue by a factor accounting for volume and surface area of a cuboid compared to a thin section.

Discussion

GABA interneurons in the PFC are integral to proper higher-order brain functions such as decision making and motivation. Understanding how GABA interneurons function at homeostasis to

regulate normal behavior will provide insight into how dysregulation could lead to mental illness or other neural problems. Molecularly characterizing different subtypes of GABA neurons and understanding their different functions through calcium imaging has been pursued by few in the field of neuroscience. Those who have attempted this characterization have done so in thin tissue sections. By optimizing methods to stain for the three major GABA neuron subtypes, SST, PV, and VIP, in thick tissue, this study provides the tools for future studies to molecularly characterize GABA neuron subtypes in thick tissue after recording their activity during behavior.

Initial failure to stain for both SST and VIP in thick tissue prompted testing of failed antibodies in thin tissue using traditional thin slice techniques. Preparing thick tissue in the exact same way as thin tissue (24 hour 4%PFA drop fix, no GA, no SDS) produced successful staining. After successful staining using traditional thin tissue techniques, the search began for the factors that were inhibiting staining in thick tissue.

Experiments showed that over-fixation with PFA was a main factor preventing staining. Cuboids fixed for 5 days in 4%PFA and then subsequently fixed in GA were used initially since this is a typical fixation duration to allow for tissue structure preservation during 6% SDS delipidation at 37°C. Since in all cases GA caused very high background compared to signal, it should not be used routinely and other fixatives should be tested in replacement. Fixation for just 24 hours in 4%PFA allowed for staining of both SST and VIP neurons. Thus for the purposes of staining GABA interneurons, this duration of fixation can be chosen and staining will be possible. In future experiments, it might be beneficial to test the effects of 48 hour and 72 hour 4%PFA fixation on SST and VIP staining since increased fixation without detriment to IHC will help to maintain tissue

integrity during clearing. It is possible that 48 hours of 4%PFA drop fix might still be compatible with SST and VIP staining but this needs to be tested under controlled conditions. Thick tissue IHC protocols often drop fix tissue in 4%PFA for between 20 hours and 3 days or use PFA/GA combinations to both preserve tissue and allow for antibody staining[15,17,34].

GA was also found to play a large role in the inhibition of thick tissue staining. As mentioned above, fixation is important to maintain shape and structure of tissue, especially in thick tissue to prevent distortion due to SDS delipidation. GA is an especially useful fixative since it is both strong and fast and thus helps maintain transgenic protein fluorescence and overall tissue integrity. Unfortunately, GA fixation often has negative impacts on IHC. It is known that GA fixation can impact the epitope of interest due to excessive cross-linking. Cross-links can mask epitopes and even change the quaternary and tertiary structure of the epitope that the antibody is meant to recognize[19,25]. Exact reactions to show how GA reacts with amine groups in tissue to change protein structure are not understood which makes it hard to know how the GA will impact the epitope of interest and how this will impact detection of an epitope through IHC[25, 32, 33].

Since it is hard to predict how GA will affect an epitope and thus IHC, it was interesting to see how differently GA affected SST and VIP staining versus PV staining. Staining a heavily GA-fixed cuboid with Mouse anti-SST H-11 did not produce any visible cell body staining. Further staining of this same cuboid with Rabbit anti-PV produced a relatively high level of cell body staining showing that GA must not be masking or destroying PV epitopes but is certainly impacting SST epitopes in some way. Since the experiment was done within the same cuboid it isolated many

confounds such that differences in staining could be attributed to GA's effects on antibody/antigen interactions.

One possible hypothesis to explain these results might be that high abundance of an antigen increases the probability of interaction between antibody and antigen in the presence of impeding cross-links. PV is known to be an abundant cytosolic calcium binding protein that can diffuse throughout the neuron to exhibit its calcium binding and moderating capacities[35,33]. SST is a neuropeptide that is stored in vesicles and released mainly from axon terminals to modulate activity of other neurons[36]. The pro form of SST, called pro-somatostatin, is made in the nucleus and is then transported down the axons to the terminals in small synaptic vesicles prior to release[36]. Interestingly, SST has been found to localize inside large dense-core vesicles in the soma, axon, and dendrites waiting to be released from these locations[33]. Overall, PV appears to be abundant and more diffuse than SST which might increase the chances of PV antibody-antigen interactions despite numerous GA induced cross-links that mask epitopes and block antibodies from accessing antigens[37,38].

Another explanation of the difference in SST and PV staining with GA could be differences in subcellular antigen location. Fixatives have been shown to have differing impacts on the ability of molecules to stain depending on cellular location. Webster et al.[39] found that antigens in the cytoplasm decrease in immunoreactivity the longer they are fixed when compared to antigens found in the cell membrane, nucleus, or extracellularly. Webster et al.[39] did not study vesicular proteins thus this finding might be an interesting addition to their data with further research. Although future research must be done to support this idea, I hypothesize that molecules in vesicles

may experience increased steric hindrance and thus have epitopes that are harder to reach. Tight packing in SST vesicles might increase steric hindrance and decrease the opportunities for correct antibody-epitope interactions. Since fixation can cause epitopes to be masked by extensive cross-linking which also creates steric hindrance, this effect might be enhanced for molecules that are present in vesicles[37,38].

To further understand how and why epitopes are affected differently by different fixatives would require an in-depth analysis of fixation chemistry and cellular localization. For now, antigen retrieval experiments[40,41] should be pursued with the SST and VIP antibodies that did not initially work in thick tissue to see if this process might unmask hidden epitopes and thus allow for antibody binding[29]. In addition, perfusion with 2% PFA has been shown by Mo et al.[42] to visualize specific VIP staining while perfusion with 4%PFA inhibited staining. In addition to trying lower fixative concentrations, less conventional fixatives like glyoxal should be tested to see if epitopes maintain immunogenicity better than when treated with GA. Glyoxal has been shown to have good fixative properties while not masking or denaturing epitopes as GA does[43]. Glyoxal has allowed for successful staining of proteins in many cellular locations such as cytoplasm, membrane, vesicular, mitochondrial, endoplasmic reticular, and Golgi apparatus[43]. Lastly, immunostaining with antibodies raised against GA treated antigens has been shown to allow for staining after GA fixation[38,37]. This would be an interesting path to pursue since GA might be necessary to preserve tissue well enough that cell alignment between in vivo imaging and ex vivo immunostaining is possible with minimal worry of SDS mediated tissue distortion.

While fixation appeared to be a major reason for lack of staining, blocking, which was initially hypothesized to have major effects on tissue staining, was shown to be unnecessary. Blocking is commonly used in thin tissue staining as a means to prevent non-specific interactions between antibodies and Fc receptors or other molecules in tissue samples[30]. In addition to prevention of non-specific interactions with the tissue itself, blocking is thought to prevent interactions between antibody and the container in which tissue is being incubated. Prevention of non-specific interactions decreases background signal and thus enhances signal to noise ratio of staining[29,30]. For these reasons, it makes sense to block tissue and thus blocking has been a mainstay throughout the history of IHC.

In newer thick tissue staining protocols, blocking appears to be less important since staining in conjunction with CLARITY often does not include blocking[15,17,26] suggesting that it is unnecessary. Since blocking was one of the main differences between thin tissue preparation and thick tissue preparation, I was interested in seeing if lack of staining or decreased effectiveness of staining in thick tissue was due to lack of blocking. There was no difference in average signal between blocked and non-blocked samples for both Rab anti-PV and Mouse anti-SST H-11. These results agree with recent findings that blocking may not be necessary[29,30,41]. In the future, anatomically matched cuboids should be used to replicate this finding as this would enable a fairer fluorescence comparison and also enable a fairer comparison for cell counting. It seemed in both graphs in Figure 8 that blocked tissue had a higher level of fluorescence at the surface of the tissue. This finding may be confounded by anatomical differences between blocked and non-blocked cuboids, so this experiment should be replicated in anatomically matching cuboids. Although blocking did not appear to make a difference in overall fluorescence intensity, it would be

interesting to see if a significantly larger number of cells are stained when blocking is used. All future replications of this experiment should be done with enough replicates to allow for significance testing since time and tissue constraints in this study did not allow for enough replicates to test for statistical significance of this finding.

Effects of SDS on Antibody Staining

SDS delipidation will effectively clear thick tissue of lipids preventing scattering of light as it passes through tissues. Since SDS is one of the many factors that differs between thin and thick tissue preparation, I was interested in seeing if SDS delipidation prior to staining tissue might be inhibiting staining. Depilidation after staining did not prove to be effective. Although tissue had less background signal, there was also less antibody staining showing that SDS removes antibody staining.

In previous research, SDS has been shown to elute antibodies at both high temperature[17] and low pH[28] but not at neutral pH and average body temperature of 37°C. Initially, reduced staining was thought to be due to the denaturing of fluorophores conjugated to secondary antibodies. Thus I hypothesized that addition of another round of secondary antibody might re-stain existing primary antibodies and bring back the signal. Since the number of detectable cells decreased after re-staining with secondary antibodies, it was determined that denaturing of secondary antibody fluorophores was not the main reason for decreased staining after SDS treatment. In the future, SDS-treated tissue should be re-stained with primary antibody to determine if primary antibody removal was the source of lost signal. If further treatment of these same tissues with primary antibody led to revival of staining signal, primary antibody removal at neutral pH and moderate

temperature is probably causing the decrease in signal. If addition of primary does not produce more cell body staining, then the epitopes are possibly being denatured by SDS. It would be valuable to pursue future experiments to determine if the cause of lost signal is due to elution of primary antibody at neutral pH and average temperature since current methods to elute antibody are more aggressive to tissue and decrease tissue integrity and structure after multiple staining rounds[17]. Overall, this experiment showed that using SDS after staining is not an effective method to both stain and clear tissue.

GABA Interneuron Populations

After looking at the many factors that impact thick tissue staining, I looked at the accuracy of GABA interneuron staining by comparing my findings to others who have stained for SST, PV, and VIP. Of the major GABA interneuron subtypes, PV appears to be the most abundant in the cortex with SST second most abundant, and VIP third most abundant [12,13,31,33]. These previous findings agree with the cell counting results in Figure 9 since PV appeared to be the most abundant GABA interneuron subtype and VIP appeared to be the least abundant.

The way that neurons stained differed between subtypes. Initially, the SST and VIP staining was thought to be non-specific, staining mostly the background or neuropil. Cell bodies were not clearly filled as they were when staining with PV antibodies. Further research showed that this pattern of staining SST, PV, and VIP subtypes in neural tissue has been noted multiple times[6,31,33,44]. SST neurons stain better around the cell periphery, often producing hollow cell bodies with absent dendritic staining[21,35]. PV neurons have fully stained cell bodies, and VIP neurons appear thin and granular when stained and often have lots of stained fibers in the

background[6,31,33,44]. VIP neurons in particular have staining that at first appears to be nonspecific due to the staining of wide arrays of slender axonal trees and dendrites running perpendicular to each cortical layer[44].

Transgenic Lines Support IHC Results

SST-Cre mouse lines were used to test for co-localization of SST staining with TdTom expressing SST neurons while PV-Cre mouse lines were used to test for co-localization of PV stain with TdTom expressing PV neurons. Overlap between transgenic and IHC stained populations of the same subtype was expected but no overlap was expected between transgenic and IHC stained populations of different GABAergic subtypes since research has shown that these SST and PV populations are distinct in the mouse PFC[31,45]. I did observe overlap between the IHC stained SST cells and the transgenically labelled SST cells in the SST-Cre line. I did not observe any overlap between antibody stained PV and transgenically labelled SST in the SST-Cre line. These results helped confirm that both the SST and PV staining worked as expected. Future research should focus on replication of this finding to confirm that IHC staining matches transgenic expression in most cases.

I expected the PV-Cre line to work since it has been shown to work by others using the same Pvalb-Cre mice from Jax that I used[46]. Unfortunately, the line failed to specifically label PV neurons leading to global expression of TdTom throughout the brain. These samples therefore could not be used in this project to determine efficiency of overlap between IHC stained PV neurons and transgenically labelled PV neurons. In the future, a working PV-Cre line should be

obtained in order to look at the overlap between IHC stained PV neurons and transgenically labelled PV neurons.

Double Staining for PV and SST

Successful double staining with SST and PV was achieved in 4%PFA fixed cuboids. The lack of overlap in PV and SST populations is supported by others in the field as these populations appear to be independent in the mouse cortex[5,31,32]. The way in which SST and PV neurons stain differs as described in the transgenic versus immunohistochemical labelling experiment. SST cells appear to stain around the exterior and do not fill in cell bodies, and this result is consistent in all immunohistochemical staining of SST in this study and others[6,7,31]. PV staining appears to fill in cell bodies and have less fibrous staining which is consistent throughout this experiment and others[6,31]. In the future, a VIP antibody that is not raised in Rabbit should be optimized in thick tissue such that simultaneous triple labelling can be done in thick tissue.

Concluding Remarks

Variable	Experimental Observation	Conclusion for Future Staining
PFA	Shorter drop fix led to better staining	4%PFA drop fix for 24 hours is sufficient to allow specific SST, PV, and VIP staining
GA	Led to high background fluorescence in all samples. Led to undetectable staining with SST and VIP	If possible refrain from using GA when staining for SST and VIP. GA is compatible with PV staining
SDS	SDS treatment after staining decreased signal drastically. SDS did not appear to have a huge impact on antibody penetration	SDS should not be used to clear tissue after staining since signal will diminish
Blocking	Did not appear to decrease non-specific staining	Blocking is not necessary in thick tissue protocols with SST, PV, and VIP

Table 3 | Overview of variables tested, results obtained, and suggestions for future staining.

Overall, this study demonstrated that the three major GABAergic neural subtypes, SST, PV, and VIP, can be stained for in thick tissue via optimized immunohistochemical techniques. However, there are limitations to this study. I tried to focus on testing a broad range of factors rather than focusing on one factor and creating many replicates to enhance statistically significance of data. One way more replicates could have been included in this study, with limited time and tissue, is by imaging all six sides of each cuboid to generate larger and fuller data sets for each cuboid. Imaging all six sides by rotating the tissue cuboid in the mounting chamber would increase the number of replicates and enable statistical testing with the data. The "Cuboid Method" sets up the platform for high throughput studies of factors affecting thick tissue immunostaining such that one factor can be tested in many cuboids at one time. The broad testing in this study was informative enough to allow for initial tests at molecularly identifying GABAergic subtypes that were recorded through in vivo calcium imaging. If future research using the cuboid method focuses on large scale replicate studies of the factors tested in this study, it will enable others with the knowledge to molecularly label a much broader range of neurons in thick tissue.

Citations

1. Lee, D. & Seo, H. Neural Basis of Strategic Decision Making. *Trends Neurosci.* **39,** 40–48 (2016).
2. Warden, M. R. *et al.* A prefrontal cortex–brainstem neuronal projection that controls response to behavioural challenge. *Nature* **492,** 428–432 (2012).
3. Banks, S. J., Eddy, K. T., Angstadt, M., Nathan, P. J. & Phan, K. L. Amygdala-frontal connectivity during emotion regulation. *Soc. Cogn. Affect. Neurosci.* **2,** 303–12 (2007).
4. Nieh, E. H., Kim, S.-Y., Namburi, P. & Tye, K. M. Optogenetic dissection of neural circuits underlying emotional valence and motivated behaviors. *Brain Res.* **1511,** 73–92 (2013).
5. Pinto, L. & Dan, Y. Cell-Type-Specific Activity in Prefrontal Cortex during Goal-Directed Behavior. *Neuron* **87,** 437–50 (2015).
6. Gonchar, Y., Wang, Q. & Burkhalter, A. Multiple distinct subtypes of GABAergic neurons in mouse visual cortex identified by triple immunostaining. *Front. Neuroanat.* **1,** 3 (2007).

7. Kim, Y. *et al.* Brain-wide Maps Reveal Stereotyped Cell-Type-Based Cortical Architecture and Subcortical Sexual Dimorphism. *Cell* **171,** 456–469.e22 (2017).
8. Kirkcaldie, M. T. K. Neocortex. in *The Mouse Nervous System* 52–111 (Elsevier, 2012). doi:10.1016/B978-0-12-369497-3.10004-4
9. Wang, H. L., Bogen, C., Reisine, T. & Dichter, M. Somatostatin-14 and somatostatin-28 induce opposite effects on potassium currents in rat neocortical neurons. *Proc. Natl. Acad. Sci. U. S. A.* **86,** 9616–20 (1989).
10. Quik, M., Iversen, L. L. & Bloom, S. R. Effect of vasoactive intestinal peptide (VIP) and other peptides on cAMP accumulation in rat brain. *Biochem. Pharmacol.* **27,** 2209–2213 (1978).
11. O'Hare, J. K. *et al.* Pathway-Specific Striatal Substrates for Habitual Behavior. *Neuron* **89,** 472–479 (2016).
12. Allen, W. E. *et al.* Global Representations of Goal-Directed Behavior in Distinct Cell Types of Mouse Neocortex. *Neuron* **94,** 891–907.e6 (2017).
13. Tomer, R., Ye, L., Hsueh, B. & Deisseroth, K. Advanced CLARITY for rapid and high-resolution imaging of intact tissues. *Nat. Protoc.* **9,** 1682–97 (2014).
14. Bocarsly, M. E. *et al.* Minimally invasive microendoscopy system for in vivo functional imaging of deep nuclei in the mouse brain. *Biomed. Opt. Express* **6,** 4546–56 (2015).
15. Chung, K. & Deisseroth, K. CLARITY for mapping the nervous system. *Nat. Methods* **10,** 508–513 (2013).
16. Richardson, D. S. & Lichtman, J. W. Clarifying Tissue Clearing. *Cell* **162,** 246–257 (2015).
17. Murray, E. *et al.* Simple, Scalable Proteomic Imaging for High-Dimensional Profiling of Intact Systems. *Cell* **163,** 1500–1514 (2015).
18. Renier, N. *et al.* iDISCO: a simple, rapid method to immunolabel large tissue samples for volume imaging. *Cell* **159,** 896–910 (2014).
19. Arnold, M. M. *et al.* Effects of Fixation and Tissue Processing on Immunohistochemical Demonstration of Specific Antigens. *Biotech. Histochem.* **71,** 224–230 (1996).
20. Berg, H. C. *Random walks in biology*. (Princeton University Press, 1993).
21. ISH Data :: Allen Brain Atlas: Mouse Brain. Available at: http://mouse.brain-map.org/. (Accessed: 4th April 2018)
22. Sylwestrak, E. L., Rajasethupathy, P., Wright, M. A., Jaffe, A. & Deisseroth, K. Multiplexed Intact-Tissue Transcriptional Analysis at Cellular Resolution. *Cell* **164,** 792–804 (2016).
23. Molgaard, S. *et al.* Immunofluorescent visualization of mouse interneuron subtypes. *F1000Research* **3,** 242 (2014).
24. Lai, H. M. *et al.* Rationalisation and Validation of an Acrylamide-Free Procedure in Three-Dimensional Histological Imaging. *PLoS One* **11,** e0158628 (2016).
25. Paavilainen, L. *et al.* The impact of tissue fixatives on morphology and antibody-based protein profiling in tissues and cells. *J. Histochem. Cytochem.* **58,** 237–46 (2010).
26. Richardson, D. S. & Lichtman, J. W. SnapShot: Tissue Clearing. *Cell* **171,** 496–496.e1 (2017).
27. Yu, T. *et al.* Elevated-temperature-induced acceleration of PACT clearing process of mouse brain tissue. *Sci. Rep.* **7,** 38848 (2017).
28. Pirici, D. *et al.* Antibody elution method for multiple immunohistochemistry on primary antibodies raised in the same species and of the same subtype. *J. Histochem. Cytochem.*

57, 567–75 (2009).
29. Jenvey, C. J. & Stabel, J. R. Autofluorescence and Nonspecific Immunofluorescent Labeling in Frozen Bovine Intestinal Tissue Sections: Solutions for Multicolor Immunofluorescence Experiments. *J. Histochem. Cytochem.* **65,** 531–541 (2017).
30. Buchwalow, I., Samoilova, V., Boecker, W. & Tiemann, M. Non-specific binding of antibodies in immunohistochemistry: fallacies and facts. *Sci. Rep.* **1,** 28 (2011).
31. Xu, X., Roby, K. D. & Callaway, E. M. Immunochemical characterization of inhibitory mouse cortical neurons: three chemically distinct classes of inhibitory cells. *J. Comp. Neurol.* **518,** 389–404 (2010).
32. Langer, D. & Helmchen, F. Post hoc immunostaining of GABAergic neuronal subtypes following in vivo two-photon calcium imaging in mouse neocortex. *Pflugers Arch.* **463,** 339–54 (2012).
33. Tremblay, R., Lee, S. & Rudy, B. GABAergic Interneurons in the Neocortex: From Cellular Properties to Circuits. *Neuron* **91,** 260–292 (2016).
34. Schwarz, M. K. *et al.* Fluorescent-protein stabilization and high-resolution imaging of cleared, intact mouse brains. *PLoS One* **10,** e0124650 (2015).
35. Schmidt, H., Arendt, O., Brown, E. B., Schwaller, B. & Eilers, J. Parvalbumin is freely mobile in axons, somata and nuclei of cerebellar Purkinje neurones. *J. Neurochem.* **100,** 727–735 (2007).
36. De Lima, A. D. & Morrison, J. H. Ultrastructural analysis of somatostatin-immunoreactive neurons and synapses in the temporal and occipital cortex of the macaque monkey. *J. Comp. Neurol.* **283,** 212–227 (1989).
37. Bacallao, R., Sohrab, S. & Phillips, C. Guiding Principles of Specimen Preservation for Confocal Fluorescence Microscopy. in *Handbook Of Biological Confocal Microscopy* 368–380 (Springer US, 2006). doi:10.1007/978-0-387-45524-2_18
38. Bell, P. B., Rundquist, I., Svensson, I. & Collins, V. P. Formaldehyde sensitivity of a GFAP epitope, removed by extraction of the cytoskeleton with high salt. *J. Histochem. Cytochem.* **35,** 1375–80 (1987).
39. Webster, J. D., Miller, M. A., Dusold, D. & Ramos-Vara, J. Effects of prolonged formalin fixation on diagnostic immunohistochemistry in domestic animals. *J. Histochem. Cytochem.* **57,** 753–61 (2009).
40. Shi, S.-R., Cote, R. J. & Taylor, C. R. Antigen Retrieval Immunohistochemistry: Past, Present, and Future. *J. Histochem. Cytochem.* **45,** 327–343 (1997).
41. Akbar, H. & Riberio, D. Antigen retrieval, blocking, detection and visualisation systems in immunohistochemistry: A review and practical evaluation of tyramide and rolling circle amplification systems. *Methods* **70,** 28–33 (2014).
42. Mo, A. *et al.* Epigenomic Signatures of Neuronal Diversity in the Mammalian Brain. *Neuron* **86,** 1369–84 (2015).
43. Richter, K. N. *et al.* Glyoxal as an alternative fixative to formaldehyde in immunostaining and super-resolution microscopy. *EMBO J.* **37,** 139–159 (2018).
44. Prönneke, A. *et al.* Characterizing VIP Neurons in the Barrel Cortex of VIPcre/tdTomato Mice Reveals Layer-Specific Differences. *Cereb. Cortex* **25,** 4854–68 (2015).
45. Bohannon, A. S. & Hablitz, J. J. Optogenetic dissection of roles of specific cortical interneuron subtypes in GABAergic network synchronization. *J. Physiol.* **596,** 901–919 (2018).
46. Kaiser, T., Ting, J. T., Monteiro, P. & Feng, G. Transgenic labeling of parvalbumin-

expressing neurons with tdTomato. *Neuroscience* **321,** 236–245 (2016).